

A SOLID ELECTROLYTE SEPARATOR FOR PULSE- POWER BATTERIES

Shyam D. Argade, P.I.
Ashok K. Saraswat
Abdessadek Lachgar (WFU)

Technochem Company
203-A Creek Ridge Road
Greensboro, NC 27406

February 1996

Final Report

Distribution authorized to DoD components only, Proprietary Information; February 1996. Other requests for this document shall be referred to AFMC/STI.

WARNING - This document contains technical data whose export is restricted by the Arms Export Control Act (Title 22, U.S.C., Sec 2751 et seq.) or The Export Administration Act of 1979, as amended (Title 50, U.S.C., App. 2401, et seq.). Violations of these export laws are subject to severe criminal penalties. Disseminate IAW the provisions of DoD Directive 5230.25 and AFI 61-204.

DESTRUCTION NOTICE - For classified documents, follow the procedures in DoD 5200.22-M, Industrial Security Manual, Section II-19 or DoD 5200.1-R, Information Security Program Regulation, Chapter IX. For unclassified, limited documents, destroy by any method that will prevent disclosure of contents or reconstruction of the document.



PHILLIPS LABORATORY
Space and Missiles Technology Directorate
AIR FORCE MATERIEL COMMAND
KIRTLAND AIR FORCE BASE, NM 87117-5776

DTIC QUALITY INSPECTED 3

19960607 079

UNCLASSIFIED



AD NUMBER

AD-B211043

NEW LIMITATION CHANGE

TO

DISTRIBUTION STATEMENT A -
Approved for public release; Distribution unlimited.

Limitation Code: 1

FROM

DISTRIBUTION STATEMENT -

Limitation Code:

AUTHORITY

Janet E. Mosher; Phillips Lab/CA, Kirtland AFB,
N.M.

THIS PAGE IS UNCLASSIFIED

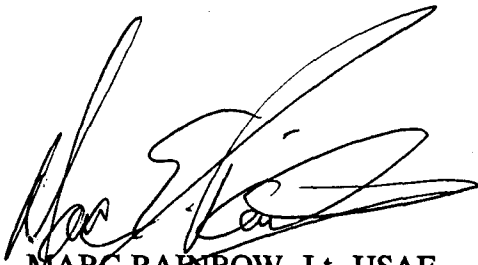
Using Government drawings, specifications, or other data included in this document for any purpose other than Government procurement does not in any way obligate the U.S. Government. The fact that the Government formulated or supplied the drawings, specifications, or other data, does not license the holder or any other person or corporation; or convey any rights or permission to manufacture, use, or sell any patented invention that may relate to them.

This report contains proprietary information and shall not be either released outside the government, or used, duplicated or disclosed in whole or in part for manufacture or procurement, without the written permission of the contractor. This legend shall be marked on any reproduction hereof in whole or in part.

If you change your address, wish to be removed from this mailing list, or your organization no longer employs the addressee, please notify PL/VTP, 3550 Aberdeen Ave SE, Kirtland AFB, NM 87117-5776.

Do not return copies of this report unless contractual obligations or notice on a specific document requires its return.

This report has been approved for publication.



MARC RAINBOW, Lt, USAF
Project Manager

FOR THE COMMANDER



DAVID H. KRISTENSEN, Lt Col, USAF
Chief, Space Power and Thermal Management
Division



HENRY L. PUGH, JR., Col, USAF
Director, Space and Missiles Technology
Directorate

The following notice applies to any unclassified (including originally classified and now declassified) technical reports released to "qualified U.S. contractors" under the provisions of DoD Directive 5230.25, Withholding of Unclassified Technical Data From Public Disclosure.

NOTICE TO ACCOMPANY THE DISSEMINATION OF EXPORT-CONTROLLED TECHNICAL DATA

1. Export of information contained herein, which includes, in some circumstances, release to foreign nationals within the United States, without first obtaining approval or license from the Department of State for items controlled by the International Traffic in Arms Regulations (ITAR), or the Department of Commerce for items controlled by the Export Administration Regulations (EAR), may constitute a violation of law.
2. Under 22 U.S.C. 2778 the penalty for unlawful export of items or information controlled under the ITAR is up to two years imprisonment, or a fine of \$100,000, or both. Under 50 U.S.C., Appendix 2410, the penalty for unlawful export of items or information controlled under the EAR is a fine of up to \$1,000,000, or five times the value of the exports, whichever is greater; or for an individual, imprisonment of up to 10 years, or a fine of up to \$250,000, or both.
3. In accordance with your certification that establishes you as a "qualified U.S. Contractor", unauthorized dissemination of this information is prohibited and may result in disqualification as a qualified U.S. contractor, and may be considered in determining your eligibility for future contracts with the Department of Defense.
4. The U.S. Government assumes no liability for direct patent infringement, or contributory patent infringement or misuse of technical data.
5. The U.S. Government does not warrant the adequacy, accuracy, currency, or completeness of the technical data.
6. The U.S. Government assumes no liability for loss, damage, or injury resulting from manufacture or use for any purpose of any product, article, system, or material involving reliance upon any or all technical data furnished in response to the request for technical data.
7. If the technical data furnished by the Government will be used for commercial manufacturing or other profit potential, a license for such use may be necessary. Any payments made in support of the request for data do not include or involve any license rights.
8. A copy of this notice shall be provided with any partial or complete reproduction of these data that are provided to qualified U.S. contractors.

D E S T R U C T I O N N O T I C E

For classified documents, follow the procedures in DoD 5200.22-M, Industrial Security Manual, Section II-19 or DoD 5200.1-R, Information Security Program Regulation, Chapter IX. For unclassified, limited documents, destroy by any method that will prevent disclosure of contents or reconstruction of the document.

DRAFT SF 298

1. Report Date (dd-mm-yy) February 1996		2. Report Type Final		3. Dates covered (from... to) 06/94 to 12/94	
4. Title & subtitle A Solid Electrolyte Separator for Pulse-Power Batteries			5a. Contract or Grant # F29601-94-C-0134		
			5b. Program Element # 62601F		
6. Author(s) Shyam D. Argade, P.I. Ashok K. Saraswat Abdessadek Lachgar (WFU)			5c. Project # 1602		
			5d. Task # C0		
			5e. Work Unit # ED		
7. Performing Organization Name & Address Technochem Company 203-A Creek Ridge Road Greensboro, NC 27406-4419				8. Performing Organization Report #	
9. Sponsoring/Monitoring Agency Name & Address Phillips Laboratory 3550 Aberdeen Ave SE Kirtland AFB, NM 87117-5776				10. Monitor Acronym	
				11. Monitor Report # PL-TR-96-1019	
12. Distribution/Availability Statement Distribution authorized to DoD components only; Proprietary Information; February 1996. Other requests shall be referred to AFMC/STI.					
13. Supplementary Notes					
14. Abstract U.S. Ballistic Missile Defense Organization (BMDO) has requirements for pulse power sources of high specific power and specific energy for applications in electric weapons, sensing, and communications systems. These objectives can be met by thin film, high temperature battery components such as a lithium-insertion anode, a lithium intercalation cathode and a high conducting Li ⁺ ion electrolyte separator. This Phase I program focussed on a new class of Li ⁺ ion conducting compounds and solid electrolytes made from these compounds using polymer gels. The inorganic Li ⁺ conductors, which are excellent gel formers, have interesting crystal structures and are thermally and electrochemically stable. The electrolyte separators of 100-200 μm thickness, made from these inorganic compounds incorporated in polymeric gels utilizing lithium salts and plasticizer-solvents, have exhibited ionic conductivity of > 5x10 ⁻³ S/cm at 100°C.					
15. Subject Terms pulse power, thin film, polymer gels.					
Security Classification of			19. Limitation of Abstract Limited	20. # of Pages 46	21. Responsible Person (Name and Telephone #) Lt Marc Rainbow (505) 846-5703
16. Report Unclassified	17. Abstract Unclassified	18. This Page Unclassified			

CONTENTS

<u>Section</u>	<u>Page</u>
1.0 INTRODUCTION	1
1.1. BACKGROUND	1
1.2. PHASE I PROGRAM	3
1.3. REPORT CONTENT	4
2.0 STUDY OF PHOSPHATOANTIMONATES	5
2.1. INTRODUCTION	5
2.2. SYNTHESIS AND CHARACTERIZATION OF $K_5Sb_5P_2O_{20}$ and $KSbP_2O_8$	5
2.3. ACID DERIVATIVES OF $KSbP_2O_8$, $K_3Sb_3P_2O_{14}$, $K_5Sb_5P_2O_{20}$	6
2.4. SYNTHESIS AND CHARACTERIZATION OF $LiSbP_2O_8$, $Li_3Sb_3P_2O_{14}$, and $Li_5Sb_5P_2O_{20}$	7
2.4.1. $LiSbP_2O_8$	7
2.4.2. $Li_3Sb_3P_2O_{14}$	7
2.4.3. $Li_5Sb_5P_2O_{20}$	8
2.5. THERMAL STABILITY OF LITHIUM PHOSPHATOANTIMONATE COMPOUNDS	8
2.5.1 $Li_3Sb_3P_2O_{14} \cdot 10H_2O$	8
2.5.2 Thermal Stability of $LiSbP_2O_8 \cdot 2.3H_2O$	9
2.5.3 Thermal Stability of $Li_5Sb_5P_2O_{20} \cdot 5.6H_2O$	9
2.5.4 Crystallographic Parameters of Anhydrous Li-Phosphatoantimonates	9
2.6. CONDUCTIVITY BEHAVIOR OF SOLID ELECTROLYTES	9
2.6.1. Preparation of Solid Electrolyte Wafers	10
2.6.2. Preparation of Silver Electrodes	10
2.6.3. Conductivity Cell Design	11
2.6.4. Conductivity Measurements	11
2.7. CONCLUSIONS - STUDY OF PHOSPHATOANTIMONATE COMPOUNDS	16
3.0 CONDUCTIVITY IMPROVEMENT SCHEMES	17
3.1. INTRODUCTION	17

3.2. ADDITION OF INORGANIC PARTICULATES	17
3.3. SUBSTITUTION OF Nb & Sb IN PHOSPHATOANTIMONATES	18
3.4. SOLID ELECTROLYTES USING POLYMER MATRICES	18
3.4.1 PVDF-Based Electrolyte Films	19
3.4.2. PAN Based Polymer Electrolyte	21
3.5. CYCLIC VOLTAMMETRY RESULTS OF $\text{Li}_5\text{Sb}_5\text{P}_2\text{O}_{20}$	25
3.6. PERFORMANCE PROJECTION	27
3.7. CONCLUSIONS - CONDUCTIVITY IMPROVEMENT SCHEMES	29
4.0 CONCLUSIONS AND RECOMMENDATIONS	31
REFERENCES	33

FIGURES

<u>Figure</u>	<u>Page</u>
1. Schematic of the cell test fixture for conductivity measurements.	12
2. The conductivity behavior of KSbP_2O_8 with temperature, as an Arrhenius plot.	14
3. Conductivity as a function of temperature as Arrhenius plot for $\text{K}_3\text{Sb}_3\text{P}_2\text{O}_{14}$	14
4. Conductivity as a function of temperature as Arrhenius plot for $\text{K}_5\text{Sb}_5\text{P}_2\text{O}_{20}$	14
5. The conductivity behavior of LiSbP_2O_8 with temperature, as an Arrhenius plot.	15
6. Conductivity as a function of temperature as Arrhenius plot for $\text{Li}_3\text{Sb}_3\text{P}_2\text{O}_{14}$	15
7. Conductivity as a function of temperature as Arrhenius plot for $\text{Li}_5\text{Sb}_5\text{P}_2\text{O}_{20}$	16
9. Arrhenius plot of conductivity for film produced from for formulation PA2	24
10. Conductivity as a function of temperature, as an Arrhenius plot, for the film of formulation PA3	25
11. Cyclic voltammogram using 1 cm^2 area platinum counter and working electrodes and a lithium reference electrode in a solution of $\text{LiN}-(\text{SO}_2\text{CF}_3)_2$ in a solvent mix of γ -butyrolactone, dibutyl phthalate, ethylene carbonate and 3-methyl-2-oxazolidinone	26
12. Cyclic voltammogram using 1 cm^2 area platinum counter and working electrodes and a lithium reference electrode in a solution of $\text{LiN}-(\text{SO}_2\text{CF}_3)_2$ in a solvent mix of γ -butyrolactone, dibutyl phthalate, ethylene carbonate and 3-methyl-2-oxazolidinone, containing a dispersion of $\text{Li}_5\text{Sb}_5\text{P}_2\text{O}_{20}$	26
13. Cell voltage versus current density for a projected 500 cm^2 area cell with a 200 ohm cm resistivity electrolyte assuming a cell polarization of $2 \times \text{IR}$ for the three thicknesses of the electrolyte separator	28
14. Projected power performance for an 8-cell bipolar 24-V $\text{Li}_x\text{C}/\text{MnO}_2$ battery system using 200 ohm cm resistivity electrolyte separators of three different thicknesses, assuming a cell polarization of twice the IR-drop	28

TABLES

<u>Tables</u>	<u>Page</u>
1. Crystallographic parameters of KSbP_2O_8 , $\text{K}_3\text{Sb}_3\text{P}_2\text{O}_{14}$, and $\text{K}_5\text{Sb}_5\text{P}_2\text{O}_{20}$	6
2. EDAX Quantitative analyses of phosphatoantimonates	6
3. Crystallographic Cell Parameters of Lithium Phosphatoantimonates	8
4. Crystallographic Cell Parameters of Phosphatoantimonates	10
5. High Temperature Conductivities of Potassium Phosphatoantimonates	12
6. High Temperature Conductivities of Lithium Phosphatoantimonates	13
7. Projected weights and thicknesses of 500 cm^2 area cell electrodes and components	27
8. Conductivity values for electrolyte separators of various combinations	30

EXECUTIVE SUMMARY

Ballistic Missile Defense Organization (BMDO) has a need for a wide spectrum of power sources for burst power, sustained power and power communications, tracking and sensing systems aboard unmanned spacecraft of future missions. The burst pulse power and sustained power requirements cannot be met by current ambient temperature batteries. High temperatures enhance electrode reaction rates to support high power densities which are essential in BMDO applications. High temperature Li/CoS₂ and Li/FeS₂ batteries operating at 450°C have shown some promise for pulse power batteries for the US Army electric weapon applications.

The objective of this technical effort is to develop a thin battery separator using thermally stable Li⁺ ion conducting phosphoantimonate membranes. These materials have stable crystal structures and are quite robust for the intended application. Thus, their application as a thin film battery separator was evaluated in this effort. This was accomplished by synthesizing candidate Li phosphoantimonate compounds, fabricating thin battery separator membranes from these materials, characterizing the properties of the battery separator electrolytes, and demonstrating improved performance of these separators for a suitable lithium battery chemistry. Technical challenges that faced this effort were potential obstacles such as could robust membranes be made from the proposed materials, would the electronic versus ionic conductivity of these membranes be favorable, would there be significant performance improvements in terms of the chosen lithium battery chemistry, would these materials be stable in contact with lithium or lithium insertion compounds.

The results of this program have been quite promising. The new Li⁺ ion conductors based on lithium phosphoantimonates have been developed with high purity and good yield. The phosphoantimonate compounds of potassium can be synthesized by a solid-state reaction, yielding compounds with interesting crystal structures for ion exchange and ionic conduction. The corresponding lithium salts of these compounds cannot be synthesized with a solid-state reaction, however, these lithium salts retain the same crystal structure habits as that of the potassium salts with minor variations. These lithium salts exhibit linear behavior for conductivity with temperature, culminating with a conductivity of 3×10^{-3} s/cm. Ionic conductivity of these salts decrease as the number of antimony atoms per compound decrease. The lithium phosphoantimonates, Li₅Sb₅P₂O₂₀ in particular, were found suitable for batteries that operate at 400 - 500°C. The use of the afore mentioned salt and supporting electrolyte in a polymer matrix looks quite promising as an electrolyte separator for lithium ion batteries. The payoff of this system would be a performance projection based on a 24 V, 500 cm² active area Li_xC/MnO₂ battery using the developed electrolyte separators is estimated to deliver a specific energy of 333 Wh/kg and an energy density of 400 Wh/l.

One of the first recommendations for the future of this technology would be to fabricate a superior lithium pulse power battery utilizing an optimized thin film electrolyte of high conductivity, in combination with a high rate lithium intercalation anode, and a suitable MnO₂ cathode. Therefore, the Phase I developments need to be further optimized, and design, develop, fabricate, and test-validate the cells and prototypes in a Phase II program.

SECTION 1

INTRODUCTION

1.1. BACKGROUND

Ballistic Missile Defense Organization (BMDO) has a need for a wide spectrum of power sources for burst power, sustained power and power for communications, tracking and sensing systems aboard unmanned spacecraft of future missions. The burst pulse power and sustained power requirements cannot be met by ambient temperature batteries. High temperatures enhance electrode reaction rates to support high power densities which are essential in BMDO applications. High temperature Li/CoS₂ and Li/FeS₂ batteries operating at 450°C have shown some promise for pulse power batteries for the US Army electric weapon applications.

The high temperature batteries exemplified above utilize immobilized molten-salt separators between the battery electrodes. The paste-like separators in operation are subject to thinning out due to electrode expansion, causing performance instabilities. Further, metallic lithium can dissolve in the molten salt causing a cell self discharge. Stable performance and long life can be achieved by using Li-intercalation electrodes and Li⁺ ion conducting solid electrolytes. Significant performance improvement is feasible by using these concepts with bipolar battery configuration and exceedingly thin cell components. Recently, feasibility of this approach has been demonstrated in TiS₂/LiAlCl₄/Li_xCoO₂ and Li-alloy/LiGeV oxides/TiS₂ batteries operating at 300°C. (References 1-2) However, the high temperature battery systems operating at much above 200°C suffer from three major disadvantages: (i) Thermal management of the system to maintain the battery at the operating temperature is very complicated; (ii) Sealing materials for cell to cell joints are rather limited and sealing to protect the cell stack assembly and the battery chemistry from the ambient environment is a difficult problem; and (iii) Operation of the battery system at high temperatures tends to lower the cycle life of these systems.

On the contrary, the ambient or room temperature Li-ion batteries are usually limited to low-rate applications. It is of interest to take advantage of the high rate capability and high electrolyte conductivity offered by higher temperatures and the thin film bipolar configurations to develop burst pulse power batteries for BMDO. In this context, pulse power batteries that operate in the intermediate temperature range of 75-150°C instead of 300-600°C should be of considerable interest for BMDO applications. Such a development would minimize the thermal management, sealing materials and cycle life problems associated with the operation of the batteries at 300-600°C. Key to this effort is the development of thin film solid electrolytes that have adequate stability and electrolytic conductivity at 75-150°C. Synthesis and characterization of new inorganic and organic solid electrolytes and their characterization are investigated as part of this SBIR Phase I R&D Program.

A number of new inorganic materials have been identified which exhibit ionic conductivities. Among those compounds are glassy Li_5AlO_4 , LiAlCl_4 , $\text{Li}_9\text{N}_2\text{Cl}_3$, $\text{Li}_{14}\text{Zn}(\text{GeO}_4)_4$ ("lisicon"), lithium silicate phosphate solid solutions and $\text{LiAl}_{11}\text{O}_{17}$ (Li- β alumina) (References 3-11). The Major disadvantages in view of practical applications of these Li ion conductors are the low thermodynamic decomposition voltage, and the formation of electrically short circuiting metallic dendrites. (References 12-13). A new group of compounds based on alkali metal phosphatoantimonates have been synthesized with interesting crystal structures which potentially can serve as ionic conductors (References 14-21).

In the organic solid electrolyte area, a number of new polymer gel electrolytes have been proposed for use in lithium batteries. These polymer gel electrolytes mainly comprise of spatial macromolecular networks, salts and organic solvents (References 22-28). On a macroscopic scale the gel behaves like a solid in which the three dimensional network participates in the deformation process. However, on a microscopic scale in which ion diffusion processes are considered, the gel behaves like a liquid. The most commonly used plasticizers / solvents include ethylene carbonate (EC), propylene carbonate (PC), γ -butyrolactone (γ BL), N, N-dimethyl formamide (DMF), N-methylpyrrolidone (NMP). Several polymer matrices have been plasticized to obtain a conductivity of the order of 10^{-3} S/cm, at room temperature. These include polyethylene glycol acrylates (PGA), polyacrylonitrile (PAN), polyethylene oxide (PE), polyvinyl chloride (PVC), polyvinylidene fluoride (PV) and polymethyl methacrylate (PMMA) (References 29-31). The most extensively studied lithium electrolytes include: LiClO_4 , LiAsF_6 , LiPF_6 , $\text{LiN}(\text{CF}_3\text{SO}_2)_2$ and LiCF_3SO_3 . More recently, a further step has been accomplished with the development of Li-TFMSI derivatives. $\text{LiCR}(\text{CF}_3\text{SO}_3)_2$, where R can be a crosslink functionality (References 32-33).

In the last few years new compounds with unique structures belonging to the class of phosphatoantimonates of potassium have been synthesized. The unique approach to their synthesis as well as their ion exchange properties show these materials to be potential candidates for use as solid electrolytes. These phosphatoantimonate compounds were prepared by Dr. Lachgar, Department of Chemistry, Wake Forest University, (WFU) Winston-Salem, NC. The candidate compounds synthesized were based on $\text{K}_5\text{Sb}_5\text{P}_2\text{O}_{20}$, $\text{K}_3\text{Sb}_3\text{P}_2\text{O}_{14}$, and KSbP_2O_8 .

The compound $\text{K}_3\text{Sb}_3\text{P}_2\text{O}_{14}$ has a layered structure. The covalent layers are built up of octahedral SbO_6 sharing corners leading to a two dimensional structure analogous to the (001) plane found in the hexagonal tungstenbronzes. On each side of the layers, PO_4 tetrahedra share three of their oxygen atoms with three different SbO_6 octahedra. The fourth oxygen atom of each PO_4 tetrahedron points to the interlayer space. Each unit cell contains nine potassium ions located between the layers. These potassium ions occupy two crystallographic sites that could contain up to twelve ions.

KSbP_2O_8 has a layered structure closely related to the structure of the compounds $\text{M}^{\text{IV}}(\text{HPO}_4)_2 \cdot \text{H}_2\text{O}$ and $\text{M}^{\text{V}}\text{H}(\text{PO}_4)_2 \cdot \text{H}_2\text{O}$. The layers $(\text{SbP}_2\text{O}_8)_n$ are built up of SbO_6 octahedra and PO_4 tetrahedra sharing corners. The SbO_6 octahedra share all their six oxygen atoms with six different tetrahedra, while each tetrahedron shares three of its oxygen atoms with three different

octahedra, the fourth oxygen points toward the interlayer space. The potassium ions have a perfect octahedral coordination.

$K_5Sb_5P_2O_{20}$ has a three-dimensional structure built up of SbO_6 octahedra sharing vertices or edges, and PO_4 tetrahedra linked to the octahedral SbO_6 via their vertices. This three dimensional framework limits large interconnecting channels extending through the structure in the [001], [110], and [-110] directions wherein the potassium ions are located connected to the SbO_6 octahedral via corner sharing.

The lithium analogues of the two layered and one three-dimensional phosphatoantimonate compounds were investigated in this SBIR Phase I Program for application in solid-electrolyte battery separators.

1.2. PHASE I PROGRAM

The objective of this overall SBIR program is to develop a pulse-power, high specific-energy low-cost, and environmentally acceptable, battery system for BMDO power applications. The Phase I program focused on the development of solid electrolytes suitable for 75-150°C operation of lithium batteries utilizing new lithium phosphatoantimonate salts. The Phase I program consisted of the following tasks and subtasks:

TASK 1. PREPARATION OF CANDIDATE MATERIALS

- Subtask 1.1 Synthesize candidate lithium phosphatoantimonates
- Subtask 1.2 Characterize the materials
- Subtask 1.3 Determine thermal and conductivity behavior
- Subtask 1.4 Select an appropriate membrane

TASK 2. THIN CELL FABRICATION

- Subtask 2.1 Develop candidate electrolyte membranes
- Subtask 2.2 Develop electrode and cell structures
- Subtask 2.3 Develop the laminating techniques
- Subtask 2.4 Fabricate the cell components

TASK 3. PERFORMANCE TESTS

- Subtask 3.1 Develop the rechargeable cell test facilities
- Subtask 3.2 Establish performance parameters
- Subtask 3.3 Demonstrate stable performance
- Subtask 3.4 Reports

1.3. REPORT CONTENT

This report on the Phase I R&D activities is presented in four sections. This section has given the background information and the Phase I program originally proposed. Section 2 details the

activities related to the development of inorganic solid electrolyte materials, their high temperature characterization, thermal stability and conductivity behavior, Section 3 discusses investigations related to conductivity improvements, and a performance projection for a Li-MnO₂ system. Section 4 provides the conclusions and recommendations of this Phase I Program.

SECTION 2

STUDY OF PHOSPHATOANTIMONATES

2.1. INTRODUCTION

In the last few years new phosphates have been synthesized, belonging to the class of phosphatoantimonates, via a unique approach to their synthesis. Preliminary studies of their crystal structures and ion exchange properties indicate that these materials potentially will have use in solid electrolytes for rechargeable lithium batteries for BMDO applications. In the Phase I program, the potassium salts of these compounds have been synthesized and converted to corresponding lithium salts, since the lithium salts of the same structures cannot be synthesized by a direct reaction of the starting components. In this section, the synthesis and characterization of these compounds are discussed.

The phosphato compounds were prepared in Dr. Lachgar's group, Department of Chemistry, Wake Forest University, (WFU) Winston-Salem, NC under a subcontract to Technochem Company. The candidate compounds synthesized were based on $K_5Sb_5P_2O_{20}$, $K_3Sb_3P_2O_{14}$ and $KSbP_2O_8$. Similar compounds, niobium analogs of antimony, $K_5Nb_5P_2O_{20}$, $K_3Nb_3P_2O_{14}$ and $KNbP_2O_8$ were produced at a later date. These potassium salts were converted to the corresponding acids, followed by an ion exchange with lithium ions to produce the respective lithium salts. These materials were characterized at Wake Forest University by x-ray powder diffraction, atomic absorption spectroscopy and electron microscopy. Electrical conductivity characterization of the potassium, and the lithium salts of these compounds were carried out at Technochem.

2.2. SYNTHESIS AND CHARACTERIZATION OF $K_5Sb_5P_2O_{20}$, $K_3Sb_3P_2O_{14}$, and $KSbP_2O_8$

Small batches of the two potassium phosphatoantimonate compounds, $K_3Sb_3P_2O_{14}$ and $K_5Sb_5P_2O_{20}$ were synthesized using the high temperature solid-state reaction process. These compounds were prepared using KNO_3 , $(NH_4)_2HPO_4$ and Sb_2O_3 as starting materials. Synthesis of $KSbP_2O_8$ was attempted using $(NH_4)_2HPO_4$. Although this synthetic method yielded the desired $KSbP_2O_8$ phase, it was difficult to separate the product from the platinum crucible. It is likely that during the decomposition, the diammonium hydrogen phosphate reacted slightly with the platinum crucible surface and consequently the ceramic phosphate could not be easily separated from the surface of the crucible. Use of ammonium dihydrogen phosphate as a source of phosphate groups turned out to be the right choice and a well crystallized $KSbP_2O_8$ was obtained. The well-ground and well-mixed materials were heated in platinum crucible initially at $200^\circ C$, followed by heating at $600^\circ C$ and finally at $900^\circ C$ for several days.

Table 1 summarizes the crystallographic information about the three potassium phosphatoantimonate compounds. Microprobe analysis using the scanning electron microscope and the energy dispersive x-ray analysis (EDAX) yielded the quantitative analysis summarized in Table 2.

Table 1 Crystallographic parameters of KSbP_2O_8 , $\text{K}_3\text{Sb}_3\text{P}_2\text{O}_{14}$ and $\text{K}_5\text{Sb}_5\text{P}_2\text{O}_{20}$.

Compound	KSbP_2O_8	$\text{K}_3\text{Sb}_3\text{P}_2\text{O}_{14}$	$\text{K}_5\text{Sb}_5\text{P}_2\text{O}_{20}$
Symmetry	Rhombohedral	Rhombohedral	Orthorhombic
a (Å)	4.7623(4)	7.147(1)	23.443(5)
b (Å)			18.452(5)
c (Å)	25.409(4)	30.936(6)	7.149(1)
V (Å ³)	499.1	1368.6	3092.5
D _{calc}	3.501	2.883	3.821
Z	3	3	6
Space Group	R-3	R-3m	Pnnm

Table 2. EDAX Quantitative analyses of phosphatoantimonates

% Mass	KSbP_2O_8				$\text{K}_3\text{Sb}_3\text{P}_2\text{O}_{14}$				$\text{K}_5\text{Sb}_5\text{P}_2\text{O}_{20}$			
	K	Sb	P	O	K	Sb	P	O	K	Sb	P	O
Calc	11	35	18	37	15	48	8.1	29	17	51	5.2	27
Expt.	11	35	18	36	16	46	8.1	30	16	50	5.5	29

In all cases the yield was 100% as determined by atomic absorption spectroscopy, electron microprobe analysis and powder x-ray diffraction of larger samples. A number of small batches taken from well-ground and well-mixed powders proved to be identical showing the repeatability of the process. The structural characterization of the materials was accomplished through x-ray powder diffraction using an automated vertical X-ray powder diffractometer equipped with a Seifert X-ray tube with a copper anode. All the diffraction peaks were indexed using the PPLP utility of the NRCVAX x-ray structure analysis package.

2.3. ACID DERIVATIVES OF KSbP_2O_8 , $\text{K}_3\text{Sb}_3\text{P}_2\text{O}_{14}$, $\text{K}_5\text{Sb}_5\text{P}_2\text{O}_{20}$

The compounds LiSbP_2O_8 , $\text{Li}_3\text{Sb}_3\text{P}_2\text{O}_{14}$, $\text{Li}_5\text{Sb}_5\text{P}_2\text{O}_{20}$ could not be directly synthesized at high temperature using LiNO_3 as a source of lithium. All the experiments to directly synthesize these compounds yielded glassy phase materials that could not be identified. The compounds LiSbP_2O_8 , $\text{Li}_3\text{Sb}_3\text{P}_2\text{O}_{14}$, $\text{Li}_5\text{Sb}_5\text{P}_2\text{O}_{20}$ were synthesized using two different techniques: (a) First method used the techniques of "chimie douce" in which the synthesis is carried out in two separate steps. The acid derivative of the potassium salt, was made followed by exchange of the protons by lithium through an acid-base titration using LiOH . (b) The second method used a molten salt for ion exchange. Results showed that both methods could yield the desired compounds but the first one

was easier to perform and was more efficient regarding the time needed for the completion. When the compounds $K_3Sb_3P_2O_8$, $K_3Sb_3P_2O_{14}$, and $K_5Sb_5P_2O_{20}$ were mixed in a strong acidic medium of 9 N HNO_3 , a complete exchange of potassium for protons occurred yielding the corresponding acid. The overall general reaction may be written as:



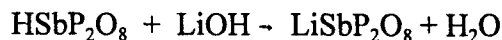
The extent of the exchange was followed by analyzing the amount of potassium in the solution as well as the amount of potassium left in the solid using atomic absorption spectroscopy and the scanning electron microscopy. X-ray analysis of the solid acids showed that the compounds conserve the structural framework of the parent potassium salt. In the case of $H_nSb_nP_2O_{3n+5} \cdot xH_2O$ the orthorhombic symmetry of $K_5Sb_5P_2O_{20}$ is conserved. For the two layered acids $HSbP_2O_8 \cdot xH_2O$ and $H_3Sb_3P_2O_{14} \cdot xH_2O$, electron diffraction studies showed that the layers $(SbP_2O_8^{-1})_n$ and $(Sb_3P_2O_{14}^{-3})_n$ are maintained.

2.4. SYNTHESIS AND CHARACTERIZATION OF $LiSbP_2O_8$, $Li_3Sb_3P_2O_{14}$, and $Li_5Sb_5P_2O_{20}$

As mentioned above, these compounds, $LiSbP_2O_8$, $Li_3Sb_3P_2O_{14}$, $Li_5Sb_5P_2O_{20}$ could not be directly synthesized at high temperature using $LiNO_3$ as a source of lithium. Lithium compounds of the requisite structures could only be obtained by the route of $K(PA) \rightarrow H(PA) \rightarrow Li(PA)$, where PA stands for phosphatoantimonate.

2.4.1. $LiSbP_2O_8$

This was prepared by exchanging protons by Li^+ cations, and is accomplished by direct acid-base titration by the following reaction:



The powder X-ray diffraction of the product $LiSbP_2O_8$ showed a similar pattern to that of $HSbP_2O_8$ and $KSbP_2O_8$. The peak positions in the diffraction pattern for $LiSbP_2O_8$ were between the corresponding peak positions of $HSbP_2O_8$ and $KSbP_2O_8$.

2.4.2. $Li_3Sb_3P_2O_{14}$

The route $K_3Sb_3P_2O_{14} \rightarrow H_3Sb_3P_2O_{14} \rightarrow Li_3Sb_3P_2O_{14}$ was also successful in the preparation of this compound. Both $NH_4H_2PO_4$ and $(NH_4)_2HPO_4$ were good starting materials as a source for phosphorus to obtain $K_3Sb_3P_2O_{14}$. The product was analyzed by x-ray powder diffraction and SEM. The X-ray powder pattern showed a spectrum that is in good agreement with the calculated one, and the SEM analysis confirmed the elemental composition of the product. The transformation of $K_3Sb_3P_2O_{14}$ into $Li_3Sb_3P_2O_{14}$ was made in concentrated HNO_3 . The product $Li_3Sb_3P_2O_{14}$ had a powder diffraction pattern similar to that of $K_3Sb_3P_2O_{14}$. SEM analysis showed no significant amount of K in the product, confirming that a complete exchange had been achieved.

2.4.3. $\text{Li}_5\text{Sb}_5\text{P}_2\text{O}_{20}$

The same processing strategy was employed for this compound: $\text{K}_5\text{Sb}_5\text{P}_2\text{O}_{20} \rightarrow \text{H}_5\text{Sb}_5\text{P}_2\text{O}_{20} \rightarrow \text{Li}_5\text{Sb}_5\text{P}_2\text{O}_{20}$. Both $\text{NH}_4\text{H}_2\text{PO}_4$ and $(\text{NH}_4)_2\text{HPO}_4$ could be used to synthesize $\text{K}_5\text{Sb}_5\text{P}_2\text{O}_{20}$. The combination of x-ray powder diffraction and SEM analysis techniques had confirmed the structure, symmetry and stoichiometry of the product. The K \rightarrow H exchange was made in concentrated HNO_3 as with other compounds. After the ion exchange procedure, the AAS analysis indicated that the K concentration in the filtrate was less than 0.5 ppm. The SEM-EDAX analysis showed no K in the product. Therefore, the ion exchange was complete. The x-ray powder pattern of $\text{H}_5\text{Sb}_5\text{P}_2\text{O}_{20}$ was very similar to that of $\text{K}_5\text{Sb}_5\text{P}_2\text{O}_{20}$. The corresponding peaks of the two compounds were almost at the same position.

LiOH solution was used in performing the titration for transforming $\text{H}_5\text{Sb}_5\text{P}_2\text{O}_{20}$ into $\text{Li}_5\text{Sb}_5\text{P}_2\text{O}_{20}$. The AAS analysis showed that there was 2.95% Li in the product (2.9% Li calculated in pure $\text{Li}_5\text{Sb}_5\text{P}_2\text{O}_{20}$) proving that the ion exchange was complete and that the product was indeed $\text{Li}_5\text{Sb}_5\text{P}_2\text{O}_{20}$. The x-ray powder diffraction patterns of $\text{K}_5\text{Sb}_5\text{P}_2\text{O}_{20}$, $\text{H}_5\text{Sb}_5\text{P}_2\text{O}_{20}$ and $\text{Li}_5\text{Sb}_5\text{P}_2\text{O}_{20}$ were almost the same. The AA analysis showed only 0.4% of Li in the product, and SEM showed the K peak in the product was the same as in $\text{K}_5\text{Sb}_5\text{P}_2\text{O}_{20}$. Hydrated lithium salts were obtained in all cases. The samples were dehydrated subsequent to TGA analysis. The crystallographic cell parameters of the hydrated lithium compounds were determined by x-ray diffraction, as presented in Table 3.

2.5. THERMAL STABILITY OF LITHIUM PHOSPHATOANTIMONATE COMPOUNDS

2.5.1. $\text{Li}_3\text{Sb}_3\text{P}_2\text{O}_{14} \cdot 10\text{H}_2\text{O}$

In order to determine the thermal stability of these compounds, thermogravimetric studies were carried out. These investigations were performed using a Perkin Elmer TGA instrument. The thermogravimetry showed that the compound contains ten water molecules per molecular formula

Table 3. Crystallographic Cell Parameters of the Lithium Phosphatoantimonates

Compound	a (Å)	b (Å)	c (Å)	β (deg.)	dint (Å)
$\text{LiSbP}_2\text{O}_8 \cdot 2.3\text{H}_2\text{O}$	4,791(3)	4,791(3)	28,20 (2)	--	≈ 9.4
$\text{Li}_3\text{Sb}_3\text{P}_2\text{O}_{14} \cdot 10\text{H}_2\text{O}$	12.49 (1)	7.22(5)	11.58(1)	107.3(1)	≈ 11.05
$\text{Li}_5\text{Sb}_5\text{P}_2\text{O}_{20} \cdot 5.6\text{H}_2\text{O}$	23.40(1)	18.51(1)	7,202(4)	--	--

at room temperature. The layered structure was maintained to 455 °C. At higher temperatures the layers collapsed and the powder diffraction became of very poor quality. The anhydrous compound corresponding to the chemical formula $\text{Li}_3\text{Sb}_3\text{P}_2\text{O}_{14}$ was obtained at 300 °C and was stable to 455 °C. At about 900 °C the compound lost oxygen and decomposed to yield SbPO_4 .

2.5.2. Thermal Stability of $\text{LiSbP}_2\text{O}_8 \cdot 2.3\text{H}_2\text{O}$

Thermogravimetric studies were combined with x-ray studies to show that the compound contained 2.3 water molecules per molecular formula, and that the structure was stable up to 480 °C. At higher temperatures the structure was destroyed and powder diffraction became of very poor quality, which did not allow determination of the symmetry and unit cell parameters of the resulting compound. The anhydrous compound corresponding to the chemical formula LiSbP_2O_8 was obtained at 180 °C, and was stable up to 480 °C. At about 900 °C the compound lost oxygen to yield SbPO_4 and $\alpha\text{-Sb}_2\text{O}_4$.

2.5.3. Thermal Stability of $\text{Li}_5\text{Sb}_5\text{P}_2\text{O}_{20} \cdot 5.6\text{H}_2\text{O}$

Thermogravimetric studies combined with x-ray studies showed that the compound contained 5.6 water molecules per molecular formula, and that the structure was stable up to 520 °C. At higher temperatures again the structure was destroyed and the powder diffraction pattern became poor in quality which did not allow to determine the symmetry and unit cell parameters of the resulting compound. The anhydrous compound corresponding to the chemical formula $\text{Li}_5\text{Sb}_5\text{P}_2\text{O}_{20}$ was obtained at 220 °C, and was stable up to 520 °C. At about 900 °C the compound lost oxygen to yield SbPO_4 and Sb_2O_4 .

2.5.4. Crystallographic Parameters of Anhydrous Lithium Phosphatoantimonates

Table 4 summarizes the results of x-ray diffraction studies, the unit cell parameters, and the interlayer spacing of the anhydrous lithium salts. Comparing the parameters in Table 3 for the hydrated salts with those for the anhydrous compounds given in Table 4, dehydration of the Li phosphatoantimonates does not appear to change the unit cell parameters to a significant degree. Comparing the data given for the corresponding potassium phosphatoantimonates, the lattice parameters are not too different indicating that crystal structures are maintained through the various transformations.

2.6. CONDUCTIVITY BEHAVIOR OF SOLID ELECTROLYTES

Conductivity studies on potassium and lithium compounds were made on 19 mm wafers. These wafers were made by a powder compaction technique. Details of wafer processing and conductivity measurements are discussed below.

Table 4 Crystallographic Cell Parameters of the Phosphatoantimonates

Compound	a (Å)	b (Å)	c (Å)	β (deg.)	dint (Å)
LiSbP_2O_8	4.67 (3)	4.67 (3)	26.0 (2)	--	≈ 7.2
$\text{Li}_3\text{Sb}_3\text{P}_2\text{O}_{14}$	--	--	--	--	≈ 6.45
$\text{Li}_5\text{Sb}_5\text{P}_2\text{O}_{20}$	22.94(1)	18.02(1)	7.18(2)	--	--

2.6.1. Preparation of Solid Electrolyte wafers

Prior to the preparation of the electrolyte wafers, to remove the residual moisture from the prepared materials, powders of phosphatoantimonate compounds were dried under vacuum. $\text{K}_5\text{Sb}_5\text{P}_2\text{O}_{20}$, $\text{K}_3\text{Sb}_3\text{P}_2\text{O}_{14}$, LiSbP_2O_8 , $\text{Li}_3\text{Sb}_3\text{P}_2\text{O}_{14}$ and $\text{Li}_5\text{Sb}_5\text{P}_2\text{O}_{20}$ powders were all dried at 300°C under dynamic vacuum for 4 hours, whereas KSbP_2O_8 was heat treated at 150°C for 4 hours in a vacuum oven. The dried powders were subsequently stored in an argon glove box..

For making wafers, powders were ground and mixed with 1-2 wt% of polyethylene oxide, PEO molecular weight of 5×10^6 , which served as a binder and lubricant. Without the binder/lubricant good wafers could not be obtained. The die, made of a hardened tool steel, was filled evenly with a preweighed amount of material in the 19 mm diameter mold cavity. The wafers were formed at 30-35 tons of load in an H-frame hydraulic press. Good quality wafers of thickness 0.35-0.75 mm were produced at 0.25-0.50 g powder weight. Wafers were baked at sufficiently high temperatures to remove the PEO lubricant, which incidentally decomposes leaving no trace behind. Wafers of KSbP_2O_8 , LiSbP_2O_8 , $\text{Li}_3\text{Sb}_3\text{P}_2\text{O}_{14}$ and $\text{Li}_5\text{Sb}_5\text{P}_2\text{O}_{20}$ were heated at 300°C for 5 hours, whereas $\text{K}_3\text{Sb}_3\text{P}_2\text{O}_{14}$ wafers were heat treated at 400°C for 4 hours. No heat treatment was given to $\text{K}_5\text{Sb}_5\text{P}_2\text{O}_{20}$ wafers. It was found that thermal stress causes the cracks in the $\text{K}_5\text{Sb}_5\text{P}_2\text{O}_{20}$ wafers. All the steps involved in wafer fabrication were performed in an argon-filled dry box.

2.6.2. Preparation of Silver Electrodes

Ion-blocking silver electrodes were used in some of the conductivity measurements and were prepared as follows: A thick slurry of silver powder (Handy Harman) was made in water. Teflon 30B emulsion from Du Pont (6 wt % of Teflon on the silver basis) was intimately mixed with the silver slurry. Addition of isopropyl alcohol to this mixture resulted in a gel, which was then uniformly spread on a 0.13 mm thick Grafoil. The silver coated Grafoil was air dried for 12 hours before heating at 450°C under nitrogen atmosphere for three hours. This procedure yielded a uniform, well adhered 0.25 mm thick silver metal coating on Grafoil. Disks of 19 mm diameter were punched out from the silver coated Grafoil and used as electrodes for conductivity measurements.

2.6.3. Conductivity Cell Design

A cell-test fixture made of nickel current collectors was used in the conductivity measurements. A nickel disc to which two 1/8" diameter nickel rods were welded served as the base. The contact electrode foil was placed on the nickel base, followed by the solid electrolyte wafer and another foil electrode. The upper current collector was placed on the contact foil to provide the electrical contact. The conductivity cell assembly was placed under compression by a spring load, which was applied externally and away from the hot zone. The entire cell assembly, shown in Figure 1, was placed inside a closed-end tube Pyrex glass enclosure. The cell assembly was carried out in an argon glove box and later was placed in a crucible furnace. A flowing argon atmosphere was maintained over the experimental cell. This arrangement allowed the direct use of calibrated leads from the impedance analyzer to minimize any stray reactance or capacitance.

2.6.4. Conductivity Measurements

The electrical behavior of solid electrolytes was investigated by *ac* impedance spectroscopy method. Samples in the form of thin wafers were sandwiched between two ion blocking electrodes. Grafoil or silver-coated Grafoil electrodes were used to achieve good electrical contact with the wafer surfaces. Preparation of these electrodes is described in Section 2.6.2. The solid electrolyte with the contacts was placed in a nickel fixture and the assembly was held under compression by a spring load, as described above. The fixture and conductivity cell with the electrolyte were placed in a glass cell. A continuous flow of argon gas was maintained during measurements. The glass cell assembly was placed in a cylindrical crucible furnace unit to study the conductivity as a function of temperature. The *ac* conductivity measurements on solid electrolytes at different temperatures were carried out using an HP 4192A LF Impedance Analyzer. Real and imaginary parts of the impedance were measured over a wide range of frequencies. Conductivities were calculated from bulk resistance values which were determined from impedance plots. In general, at higher temperatures a defined semi-circle was apparent in the complex impedance plots. The bulk resistance values were determined from the intercept of the semi circle on the real axis.

2.6.4.1. Conductivity Behavior of Potassium Phosphoantimonates Silver electrodes were used for conductivity measurements on $K_3Sb_3P_2O_{14}$ and $K_5Sb_5P_2O_{20}$ compounds. $KSbP_2O_8$ wafer was sandwiched between two Grafoil pieces for conductivity studies. Measurements on $K_3Sb_3P_2O_{14}$ and $K_5Sb_5P_2O_{20}$ were taken during cooling cycle whereas $KSbP_2O_8$ wafers were studied during heating cycle. Table 5 summarizes the results of conductivity investigation on these compounds. Arrhenius plots for conductivities of $KSbP_2O_8$, $K_3Sb_3P_2O_{14}$ and $K_5Sb_5P_2O_{20}$ are given in Figures 2, 3 and 4, respectively. In the case of $KSbP_2O_8$, it was impossible to identify bulk resistance value from the impedance plots at low temperatures near ambient because of the low ion conductivity of the material. A discontinuity in the Arrhenius curves of both of these compounds can be seen.

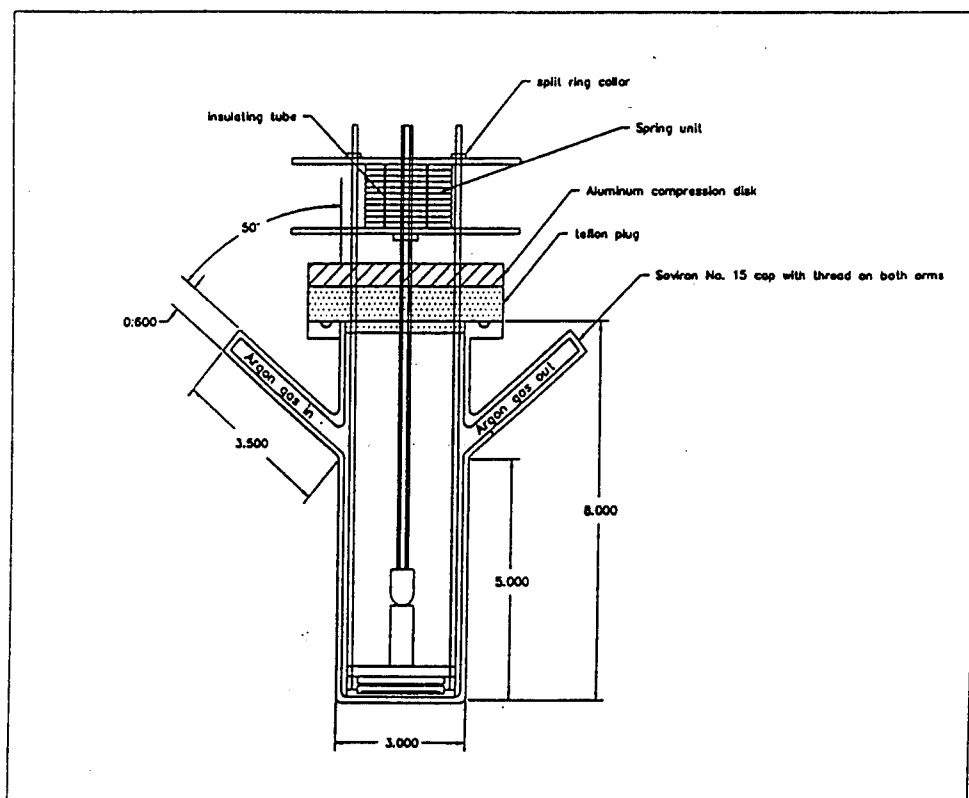


Figure 1. A schematic of the cell test fixture for conductivity measurements.

Table 5. High Temperature Conductivities of Potassium Phosphoantimonates

Compound	Thickness of Wafer (mm)	Temp. range ($^{\circ}$ C)	Max. Conductivity (S/cm)
KSbP_2O_8	0.352	27-448	2.8×10^{-6} @ 448 $^{\circ}$ C
$\text{K}_3\text{Sb}_3\text{P}_2\text{O}_{14}$	0.310	546-294	3.0×10^{-3} @ 546 $^{\circ}$ C
$\text{K}_5\text{Sb}_5\text{P}_2\text{O}_{20}$	0.750	540-117	3.8×10^{-3} @ 540 $^{\circ}$ C

Conductivity of $\text{K}_3\text{Sb}_3\text{P}_2\text{O}_{14}$ salt increases with temperature and attains a value of 3×10^{-3} (S/cm) at 546°C . Figure 4 shows the conductivity as a function of temperature as the Arrhenius plot $\text{K}_5\text{Sb}_5\text{P}_2\text{O}_{20}$ compound. A discontinuity in the Arrhenius plot can be seen for this compound as well. This compound exhibited a conductivity value of 3.8×10^{-3} S/cm at 540°C .

2.6.4.2. Conductivity Behavior of Lithium Phosphatoantimonates. Conductivity measurements on lithium phosphatoantimonate compounds were carried out in the heating cycle. Wafers were sandwiched between two Grafoils for these measurements. Table 6 summarizes results of conductivity values for these compounds. Figure 5 gives Arrhenius plot for conductivity of LiSbP_2O_8 compound. Conductivity of this compound increases almost linearly with temperature except at low temperatures where conductivity increases rather sharply. At 475°C , conductivity of this compound is 5.5×10^{-5} (S/cm). Figures 6 and 7 represent Arrhenius plots for $\text{Li}_3\text{Sb}_3\text{P}_2\text{O}_{14}$ and $\text{Li}_5\text{Sb}_5\text{P}_2\text{O}_{20}$ compounds, respectively. Conductivity of both of these compounds increases almost linearly with temperature. The maximum conductivity achieved in $\text{Li}_3\text{Sb}_3\text{P}_2\text{O}_{14}$ at 450°C is 5.4×10^{-4} S/cm whereas $\text{Li}_5\text{Sb}_5\text{P}_2\text{O}_{20}$ gives a conductivity value of 1.9×10^{-3} (S/cm) at 492°C .

Table 6. High Temperature Conductivities of Lithium Phosphatoantimonates

Compound	Thickness of Wafer (mm)	Temp. range ($^\circ\text{C}$)	Max. Conductivity (S/cm)
LiSbP_2O_8	0.351	20-494	5.5×10^{-5} @ 475°C
$\text{Li}_3\text{Sb}_3\text{P}_2\text{O}_{14}$	0.710	28-450	5.4×10^{-4} @ 450°C
$\text{Li}_5\text{Sb}_5\text{P}_2\text{O}_{20}$	0.350	19-492	1.9×10^{-3} @ 492°C

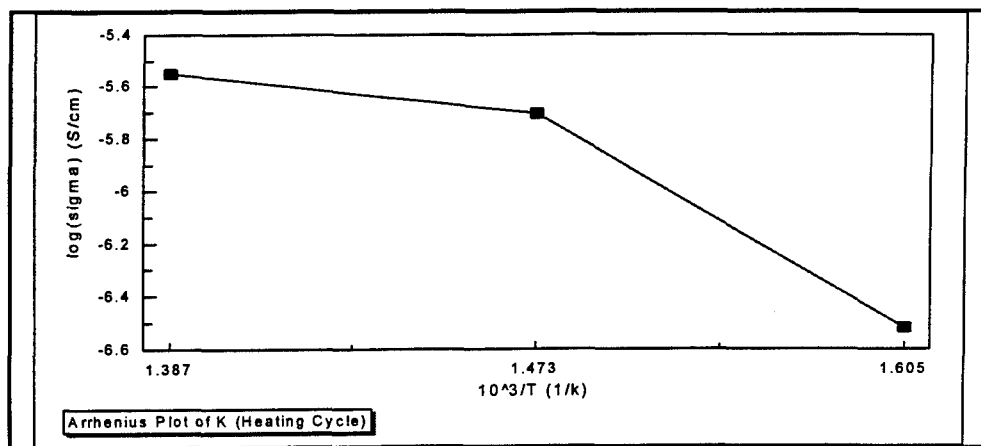


Figure 2. The conductivity behavior of KSbP_2O_8 with temperature, as an Arrhenius plot.

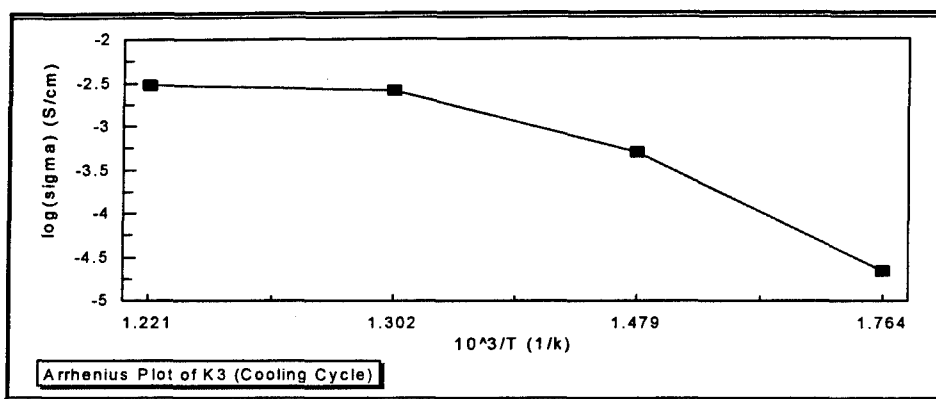


Figure 3. Conductivity as a function of temperature as Arrhenius plot for $\text{K}_3\text{Sb}_3\text{P}_2\text{O}_{14}$

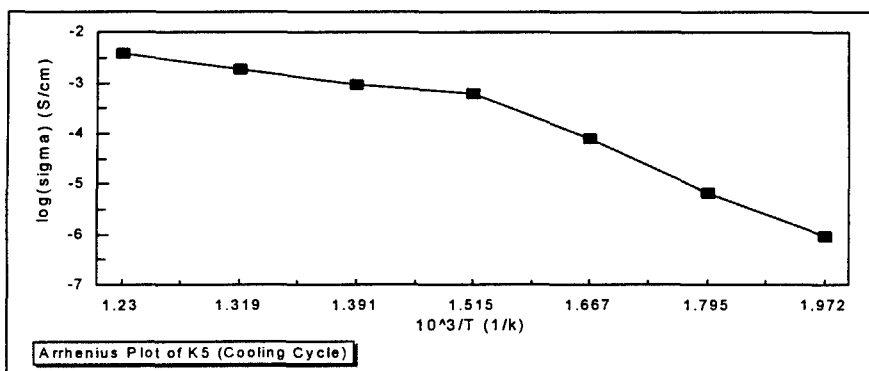


Figure 4. Conductivity as a function of temperature as Arrhenius plot for $\text{K}_5\text{Sb}_5\text{P}_2\text{O}_{20}$.

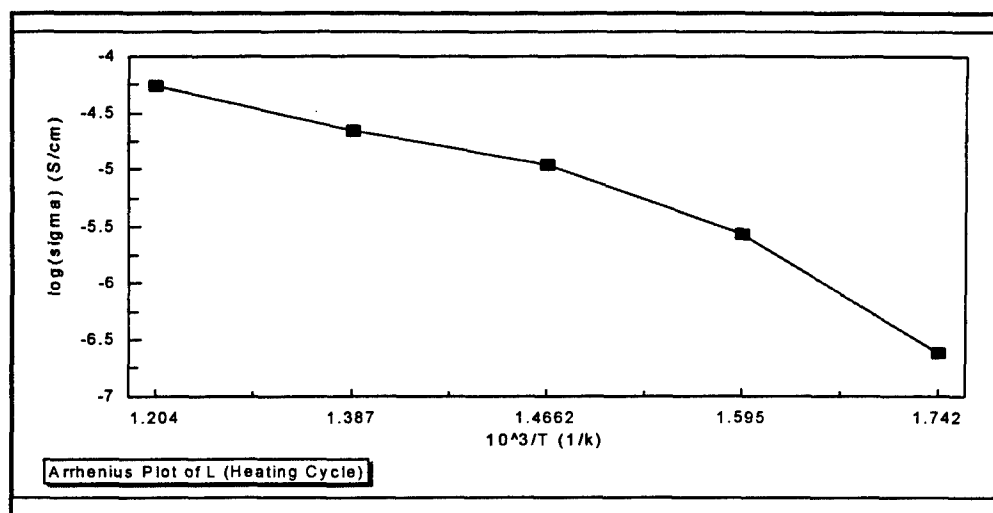


Figure 5. The conductivity behavior of LiSbP_2O_8 with temperature, as an Arrhenius plot.

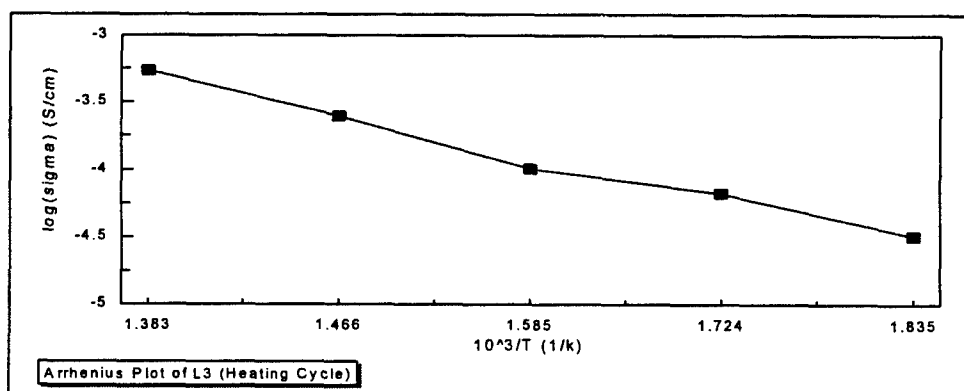


Figure 6. Conductivity as a function of temperature as Arrhenius plot for $\text{Li}_3\text{Sb}_3\text{P}_2\text{O}_{14}$.

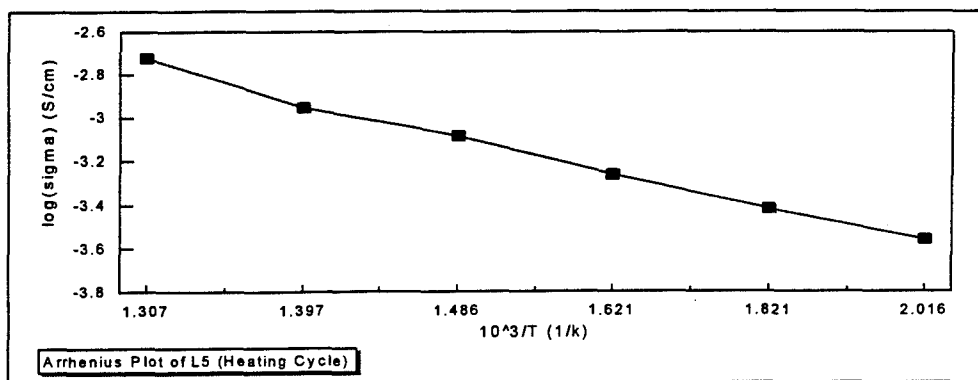


Figure 7 Conductivity as a function of temperature as Arrhenius plot for $\text{Li}_5\text{Sb}_5\text{P}_2\text{O}_{20}$

2.7. CONCLUSIONS - STUDY OF PHOSPHATOANTIMONATE COMPOUNDS

1. The phosphatoantimonate compounds of potassium, KSbP_2O_8 , $\text{K}_3\text{Sb}_3\text{P}_2\text{O}_{14}$ and $\text{K}_5\text{Sb}_5\text{P}_2\text{O}_{20}$ can be synthesized by solid-state reactions of $\text{NH}_4\text{H}_2\text{PO}_4$, KNO_3 and Sb_2O_3 in proper proportions. These compounds have interesting crystal structures for ion exchange and ionic conduction.
2. The corresponding lithium salts of these compounds cannot be prepared by solid-state reaction.
3. The potassium phosphatoantimonates can be completely converted into the corresponding acids without destruction of the crystal structure by treatment in 9 M nitric acid.
4. The lithium phosphatoantimonates can be made from the phosphatoantimonic acid by an acid-base titration. These lithium salts retain the same crystal structure habits as those for the corresponding potassium salts with minor changes in crystallographic lattice parameters.
5. The crystal structures are stable to a sufficiently high temperature.
6. Both the potassium and lithium phosphatoantimonates of three different compositions could be pressed into wafers for ionic conductivity measurements.
7. The potassium phosphatoantimonates exhibit low conductivities in the temperature range of interest and the conductivity versus $1/T$ is not linear and undergoes a change in the slope of the curve at temperatures of about 250-300°C.
8. The lithium phosphatoantimonates, Li_3 and Li_5 type, exhibit a linear behavior for conductivity with temperature. The conductivity of these materials is in the range of 3×10^{-3} S/cm.

SECTION 3

CONDUCTIVITY IMPROVEMENT SCHEMES

3.1. INTRODUCTION

The overall goal of this Phase I program is to develop an electrolyte separator for pulse-power batteries for BMDO applications. In section 2, the research efforts devoted to synthesis and characterization of an array of lithium phosphatoantimonate salts are described. As the conductivities of the lithium phosphatoantimonates are not sufficiently high, several alternatives to develop electrolyte separators of good conductivity in the range of temperatures of interest have been examined, as follows:

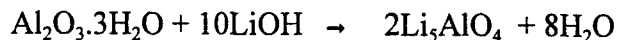
- Addition of inorganic fillers in lithium phosphatoantimonate matrix as a solid electrolyte;
- Substitution of Nb and Ge for Sb in phosphatoantimonate salts; and
- Develop a polymer matrix using phosphatoantimonate salts.

This section discusses the results of these investigations.

3.2. ADDITION OF INORGANIC PARTICULATES

Improvement of the ionic conductivity was sought via addition of inorganic high surface area particulates to a selected lithium phosphatoantimonate compound. Literature reports for other systems have indicated that the addition of high surface area particulates increased the parent matrix conductivity significantly, most likely via surface ion conduction. An inorganic filler Li_5AlO_4 was selected, being itself a Li^+ ion conductor. The Li_5AlO_4 compound was prepared as follows:

Alumina trihydrate, $\text{Al}_2\text{O}_3 \cdot 3\text{H}_2\text{O}$, (Georgia Marble Co.) and lithium hydroxide LiOH (FMC, Lithium Division) were used as received. A stoichiometric amount of alumina hydrate powder was added to water and vigorously stirred to produce a colloidal solution. A requisite amount of an aqueous LiOH solution was added under vigorous agitation to produce a white precipitate of Li_5AlO_4 . The chemical reaction may be represented as



Water from the precipitate was removed by vacuum evaporation at 100°C . This almost dried Li_5AlO_4 was heated to 550°C in air for 4 hours, and then stored in an argon-filled dry box. The Li_5AlO_4 mass was ground to a very fine powder. A 20 wt% Li_5AlO_4 was added to the dried $\text{Li}_5\text{Sb}_5\text{P}_2\text{O}_{20}$ powder and mixed well. An addition of 1 to 2 wt% of PEO to this mixture as a lubricant was found to be helpful in pelletizing the electrolyte wafers, according to the procedure outlined in Section 2. The

conductivity achieved in this solid electrolyte at 475°C is 1×10^{-3} S/cm, in the same range as the neat lithium phosphoantimonate.

3.3. SUBSTITUTION OF Nb AND Ge FOR Sb IN PHOSPHATOANTIMONATES

New materials with different stoichiometries were synthesized using two different strategies: (i) substitution of antimony by niobium in the lithium phosphoantimonates; and (ii) defect creation in the phosphoantimonate structure by partially replacing Sb(V) by Ge(IV).

(i) Direct synthesis and substitution of antimony by Nb: Three compounds in the ternary system $\text{Li}_2\text{O}-\text{Nb}_2\text{O}_5-\text{P}_2\text{O}_5$, were synthesized with stoichiometries $\text{Li}_5\text{Nb}_5\text{P}_2\text{O}_{20}$, $\text{Li}_3\text{Nb}_3\text{P}_2\text{O}_{14}$, and LiNbP_2O_8 . These compounds were synthesized at high temperatures using LiNO_3 , Nb_2O_5 , and P_2O_5 as starting materials. The compounds were made at 1050°C in platinum crucibles under a flow of oxygen. The x-ray powder diffraction pattern did not match any of the known niobates and it was complicated preventing indexation. Nevertheless, they were processed into wafers for conductivity measurements.

The $\text{Li}_5\text{Nb}_5\text{P}_2\text{O}_{20}$ and $\text{Li}_3\text{Nb}_3\text{P}_2\text{O}_{14}$ powdered materials were dried in vacuum at 300°C for 4 hours prior to use. For making wafers, powder was ground and well mixed with 1-2 wt% of PEO (M.W. $\sim 5 \times 10^6$) which served as a binder and lubricant in the mold. The wafers were made at 30-35 tons of load in an H-frame hydraulic press. The recovered wafers were heated at 250°C for two hours to burn off the organic binder. The 19 mm diameter wafers were mechanically strong at a thickness of 0.485-0.468 mm and weights of 0.5-0.55 g. Samples were sandwiched between two gold foil disks and studied for their conductivity behavior. The $\text{Li}_5\text{Nb}_5\text{P}_2\text{O}_{20}$ and $\text{Li}_3\text{Nb}_3\text{P}_2\text{O}_{14}$, gave conductivity values of 5.1×10^{-4} S/cm and 3.2×10^{-4} S/cm at 498°C, respectively.

(ii) Defect creation by substitution of some of the antimony (V) with germanium (IV): This was applied to two compounds. Two compounds of general formula $\text{Li}_{5(1+x)}\text{Ge}_x\text{Sb}_{5(1-x)}\text{P}_2\text{O}_{20}$, with $x=0.4$ and 0.8 were prepared. The $\text{Li}_9\text{Ge}_4\text{SbP}_2\text{O}_{20}$ and $\text{Li}_7\text{Ge}_2\text{Sb}_3\text{P}_2\text{O}_{20}$ powders were dried at 250°C under vacuum for 4 hours. Weighed amount of powder was mixed with 3.5 wt% of PEO. Powder was evenly filled in a mold and pressed at 25 tons of pressure. Wafers were heat treated at 250°C for 2 hours under vacuum. The recovered 19 mm diameter wafers were mechanically strong at a thickness 0.62 mm and a weight of 0.56g.

Conductivity measurements on $\text{Li}_9\text{Ge}_4\text{SbP}_2\text{O}_{20}$ and $\text{Li}_7\text{Ge}_2\text{Sb}_3\text{P}_2\text{O}_{20}$ were performed using gold blocking electrodes. $\text{Li}_9\text{Ge}_4\text{Sb}_3\text{P}_2\text{O}_{20}$ gave a conductivity value of 3.6×10^{-5} S/cm at 398°C whereas conductivity of $\text{Li}_7\text{Ge}_2\text{Sb}_3\text{P}_2\text{O}_{20}$ compound at 442°C is 3.4×10^{-5} S/cm.

3.4. SOLID ELECTROLYTES USING POLYMER MATRICES

The solid electrolytes, discussed so far, appear to have sufficient conductivities only at high temperatures. Batteries incorporating these solid electrolyte separators would operate at 400-

500°C. Lithium batteries operating in this temperature range pose several major difficulties: (i) Due to the high temperature, thermal management and maintaining the operating temperature are critical issues; (ii) Materials' problems for sealing and containment at high temperature are quite severe; (iii) The reactivity of materials is enhanced at high temperatures, and consequently, degradation of active materials is also accentuated leading to a shortened cycle life; (iv) The lithium activity in the anodes of the rechargeable lithium batteries leads to unwanted self-discharge reactions.

On the contrary, room-temperature solid-electrolyte lithium batteries, usually based on polymer-gel electrolytes, are restricted to low rate applications. If these batteries can be operated in the temperature range of 75-150°C, it will enhance the rate capabilities as well as improve the ionic conductivity of the solid electrolytes. The construction of these batteries, operating at 75-150°C, is easier and affords design flexibility by developing electrolytes of 100 μm thickness with thin electrode matrices laminated to the solid electrolyte separator. Bipolar batteries of this type can certainly meet the BMDO requirements for different power sources. These batteries should possess long cycle life with low self-discharge reactions with very high specific energy and good power density.

Thus, the approach of operation of the batteries at the intermediate temperatures would be advantageous, compared to those operating at 400-500°C. To achieve high ionic conductivity yet attain stability with thin electrolyte separators at 75-150°C, the approach of uniform dispersion of the solid electrolyte powders in a suitable polymer matrix was selected. This subsection describes the R&D efforts devoted to the development of polymer-based electrolyte separators containing the already developed phosphatoantimonate type ionic conductors. To establish the feasibility of the approach, a solid electrolyte powder was uniformly dispersed in a polymer which served as a supporting matrix. $\text{Li}_5\text{Sb}_5\text{P}_2\text{O}_{20}$ was selected because it exhibited highest conductivity among lithium phosphatoantimonate salts. Polymers, namely polyvinylidene fluoride (PVDF), and polyacrylonitrile (PAN) were selected due to their good film and gel forming properties.

3.4.1. PVDF-Based Electrolyte Films

3.4.1.1 Preparation of Electrolyte Film. PVDF polymer was used as a supporting matrix for electrolyte components. Three films of varying compositions and components were prepared. Following formulations, using the procedure given below, yielded bubble-free, free standing electrolyte films. Weights listed in the following formulations were the starting concentrations of the various components.

PV 1	PVDF (Aldrich) (MW 500,000)	3.00 g
	Dibutylphthalate (DBP) (Aldrich)	1.85
	Propylene carbonate (PC) (Texaco)	4.96
	Dimethyl formamide (DMF) (Aldrich)	1.84
	Li-bis trifluoromethanesulfonylimide(Li-TFMSI)(3M)	1.30
	$\text{Li}_5\text{Sb}_5\text{P}_2\text{O}_{20}$	0.20

PV2	PVDF	1.25 g
	DBP	0.93
	PC	2.48
	Li-TFMSI	0.65
	$\text{Li}_5\text{Sb}_5\text{P}_2\text{O}_{20}$	0.13
	Li_5AlO_4	0.13
PV3	PVDF	2.75 g
	DBP	2.25
	PC	3.62
	Ethylene carbonate(EC)(Aldrich)	1.59
	DMF	1.54
	Li-TFMSI	1.40
	$\text{Li}_5\text{Sb}_5\text{P}_2\text{O}_{20}$	0.20
	Cab-O-Sil (EH-15) (Cabot Corp.)	0.15

The specified amount of dibutyl phthalate was added to PVDF powder. Thorough mixing of these two components resulted in a thick paste to which a small amount of the PC was added. Heating at approximately 110°C for a few minutes reduced this paste into a plasticized polymer mass which was subsequently dissolved in a PC and DMF mixture. A small amount of THF was added to adjust the viscosity of the solution. After complete dissolution of the polymer, Li-TFMSI salt was added. When all the components were dissolved, a weighed amount of $\text{Li}_5\text{Sb}_5\text{P}_2\text{O}_{20}$ was added to the clear solution except for PV3 film preparation. For preparation PV3, $\text{Li}_5\text{Sb}_5\text{P}_2\text{O}_{20}$ powder was added in the mixture at the first stage. The solution was stirred for about half an hour to allow suspended $\text{Li}_5\text{Sb}_5\text{P}_2\text{O}_{20}$ particles to distribute uniformly in the solution. Weighed amount of Li_5AlO_4 powder prepared in Technochem, as described earlier, was added to the PV2 solution and stirred for half an hour. This dispersion was then poured inside a glass ring which was placed on a glass plate. After drying under ambient conditions, films were dried in a vacuum oven at 70°C for 24 hours. The dried films were then stored in an argon-filled dry box prior to measuring their ionic conductivity.

3.4.1.2 PVDF-Based Films - Results. The *ac* conductivity measurements were carried out in the manner described previously. The samples were sandwiched between gold electrodes and were kept in a nickel fixture. The assembly was held under compression by a spring load. The fixture with the electrolyte was placed in a glass cell. Cells were assembled in an argon filled dry box. Measurements were made at different temperatures during the cooling cycle. Electrical behavior of the composition PV1 was studied between 43°-140°C. The polymer film retained its shape up to 100°C. Conductivity versus temperature data were obtained for this film, as shown in Figure 8 representing an Arrhenius plot. The conductivity achieved at 140°C is 3.7×10^{-3} S/cm,

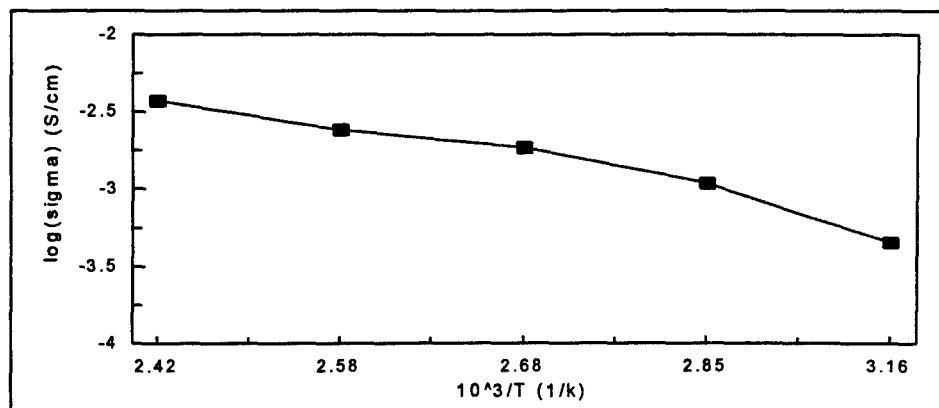


Figure 8. Conductivity versus temperature, Arrhenius plot for film of formulation PV1

although some softening and extrusion was observed at this high temperature. The preliminary investigation on this film looked quite promising and efforts were oriented to the development of an electrolyte film of improved mechanical stability and conductivity as well.

A small amount of Li_5AlO_4 was added to film PV2 during preparation. The mechanical stability of the film improved significantly by adding Li_5AlO_4 to the polymer matrix. No loss in thickness of the film was observed to 140°C . This film gave a conductivity value of 8.3×10^{-4} S/cm at 140°C .

In electrolyte film PV3, Li_5AlO_4 was replaced by a fumed silica, Cab-O-Sil. This addition of provided excellent mechanical strength to the film. However, conductivity of this film was not as high as PV1 film. This film gave a conductivity value of 4.8×10^{-4} S/cm at 100°C

3.4.2 PAN Based Polymer Electrolyte

3.4.2.1 Preparation of Electrolyte Films. Polyacrylonitrile (PAN) polymer was used as a supporting matrix for electrolyte components, as discussed below. Three films of different compositions were prepared. In these films $\text{Li}_5\text{Sb}_5\text{P}_2\text{O}_{20}$ was used in the solid form. Weights given in the following formulations are the starting concentrations of the various components.

PA 1	PAN, M.W. 150,000, (Poly Sciences)	1.75 g
	Gamma-butyrolactone, (γ BL) (Aldrich)	7.00
	EC	8.25
	PC	2.00
	MOZ (Aldrich)	1.00
	Li-TFMSI	1.98
	$\text{Li}_5\text{Sb}_5\text{P}_2\text{O}_{20}$	0.30

PA 2	PAN	0.50 g
	Gamma-BL	8.84
	EC	8.29
	PC	1.50
	MOZ	0.70
	DBP	0.54
	Li-TFMSI	0.57
	$\text{Li}_5\text{Sb}_5\text{P}_2\text{O}_{20}$	0.25
	Cab-O-Sil	0.26

PA 3	PAN	0.50 g
	Gamma-BL	8.52
	EC	6.33
	PC	2.20
	MOZ	0.79
	DBP	1.04
	Li-TFMSI	0.57
	$\text{Li}_5\text{Sb}_5\text{P}_2\text{O}_{20}$	0.25
	Cab-O-Sil	0.11

For PA1 electrolyte film preparation the PAN polymer was dissolved in γ BL + EC mixture at $\sim 110^\circ\text{C}$. EC, besides acting as a good plasticizer, also facilitates the dissolution of the polymer. After complete dissolution of the polymer Li-TFMSI was added to the above mixture. $\text{Li}_5\text{Sb}_5\text{P}_2\text{O}_{20}$ was added in the solid form. The solution was stirred for an hour before pouring inside a glass ring on a glass plate. Film was allowed to dry under ambient conditions for 10 hours. This was followed by drying in a vacuum oven at 70°C for 14 hours. Films were exposed to the ambient for a bare minimum time during transfer from the vacuum oven to an argon-filled dry box.

Film of formulation PA2 was prepared as follows: PAN polymer was dissolved in the mixture of solvents. Weighed amount of $\text{Li}_5\text{Sb}_5\text{P}_2\text{O}_{20}$ was mixed with DBP and a small amount of gamma-BL and heated slightly. Appropriate amount of Cab-O-Sil was added to this mixture and mixed thoroughly. This mixture of $\text{Li}_5\text{Sb}_5\text{P}_2\text{O}_{20}$, γ -BL, DBP and Cab-O-Sil was added to PAN solution, and stirred for an hour. Weighed amount of Li-TFMSI was dissolved in EC & gamma-BL and added to the above mixture. Cast solution was dried and handled in similar manner, as described above. Residual concentration of solvents in the film after the drying procedure was determined; and was found to be 37% of the total weight of the film.

To prepare the electrolyte film of formulation PA3, the weighed amount of $\text{Li}_5\text{Sb}_5\text{P}_2\text{O}_{20}$ salt was mixed with DBP and gamma-BL, this mixture was slightly heated. After mixing these components for an hour, a weighed amount of PAN polymer was added to this mixture. The mixture was heated to $\sim 110^\circ\text{C}$ for few minutes and stirred for about an hour. Appropriate

amount of Li-TFMSI was dissolved in EC & γ -BL and added to the above mixture. Cab-O-Sil was added to the mixture before adding MOZ. Cast solution was dried and handled in a similar manner, as discussed in PA1 film preparation procedure.

In the following film preparation, a slightly different approach was attempted to produce a high conductivity and good mechanical strength electrolyte film. Instead of using $\text{Li}_5\text{Sb}_5\text{P}_2\text{O}_{20}$ powder, the corresponding acid form of this compound was used for film preparation. The acid, $\text{H}_5\text{Sb}_5\text{P}_2\text{O}_{20}$ has good gelling properties. After vacuum drying the film of following starting concentrations of various components, it was lithiated with the help of butyl-lithium.

PA 4	PAN	0.44 g
	Gamma-BL	12.84
	PC	2.09
	EC	6.33
	MOZ	1.24
	PEG DME (PolySciences)	0.46
	Li-TFMSI	0.50
	$\text{H}_5\text{Sb}_5\text{P}_2\text{O}_{20}$	0.28

The acid, $\text{H}_5\text{Sb}_5\text{P}_2\text{O}_{20}$ was gelled in gamma-BL and EC. A few drops of water was also added to the gel solution to improve the gelification. This solution was heated at 100°C until 30-40 wt% of solvents evaporated. This solution was added to the predissolved polymer solution. After thorough mixing of these two solutions, preweighted amount of Li-TFMSI was added. MOZ and PEG DME were added in the last. This light brown solution was cast and dried at ambient conditions for four hours before placing in a vacuum oven. Temperature of the vacuum oven was raised to 70°C and films were dried for 24 hours. After drying, the films were dipped in butyl lithium solution in γ -BL for 5 hours.

3.4.2.2 PAN - Based Films - Results. Conductivity measurements were carried out on PAN-based electrolyte film by using gold blocking electrodes. Cells were assembled in an argon-filled dry box. Film of formulation PA1 showed good mechanical strength. Measurements were taken at as high as 140°C . This film retained its shape. Conductivity of this film at 140°C is $2.4 \times 10^{-3} \text{ S/cm}$. Conductivity of this film was not as high as expected, probably due to agglomeration of $\text{Li}_5\text{Sb}_5\text{P}_2\text{O}_{20}$ particles in the polymer matrix. The agglomeration resulted in a non-uniform distribution of $\text{Li}_5\text{Sb}_5\text{P}_2\text{O}_{20}$ particles in the polymer. These scattered masses in polymer matrix acted as non conducting zones and affected electrolyte conductivity adversely.

In an attempt to suppress agglomeration and facilitate the uniform distribution of the $\text{Li}_5\text{Sb}_5\text{P}_2\text{O}_{20}$ particles in polymer matrix instead of adding salt powder in solid form $\text{Li}_5\text{Sb}_5\text{P}_2\text{O}_{20}$ powder was well mixed with solvents/plasticizers such as, DBP, gamma-BL and then added to the solution. A small amount of Cab-O-Sil was added to electrolyte solution to improve the dispersion, and to enhance the film mechanical strength and conductivity as well. Two electrolyte films of formulations PA2 and PA3 were prepared using this approach. These films showed excellent

mechanical strength and no agglomeration of particles could be seen. Conductivity data as a function of temperature, shown in Figure 9, were obtained for the film PA2. This electrolyte film achieved a conductivity of 5.1×10^{-3} S/cm at 100 °C. The film from formulation PA3 gave a conductivity of 5.6×10^{-3} S/cm at 100°C, and a conductivity variation with temperature for the film of formulation PA3, as an Arrhenius plot given in Figure 10. As mentioned earlier, electrolyte film PA4 was prepared using acid form of the $\text{Li}_5\text{Sb}_5\text{P}_2\text{O}_{20}$ salt. The idea of using this approach was to take advantage of the colloidal particles of $\text{H}_5\text{Sb}_5\text{P}_2\text{O}_{20}$ and its gelling properties. The gel of $\text{H}_5\text{Sb}_5\text{P}_2\text{O}_{20}$ produced fine colloidal particles which even after lithiation did not agglomerate and remained distributed in the polymer matrix evenly. There were indications that traces of water were still present in this film. The thorough removal of water from this matrix would have to be investigated at a later date. The key objective of achieving a mechanically stable polymer electrolyte film at temperatures of upto 140°C was accomplished. These polymer films did not extrude out, although the films were held under compression in the conductivity measurement cell.

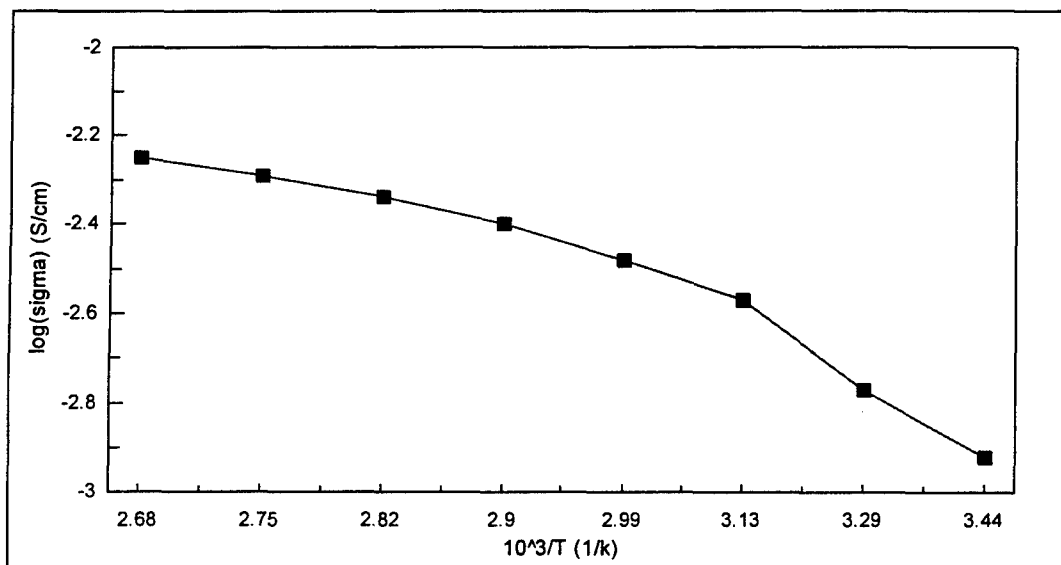


Figure 9. Arrhenius plot of conductivity for film produced from formulation PA2

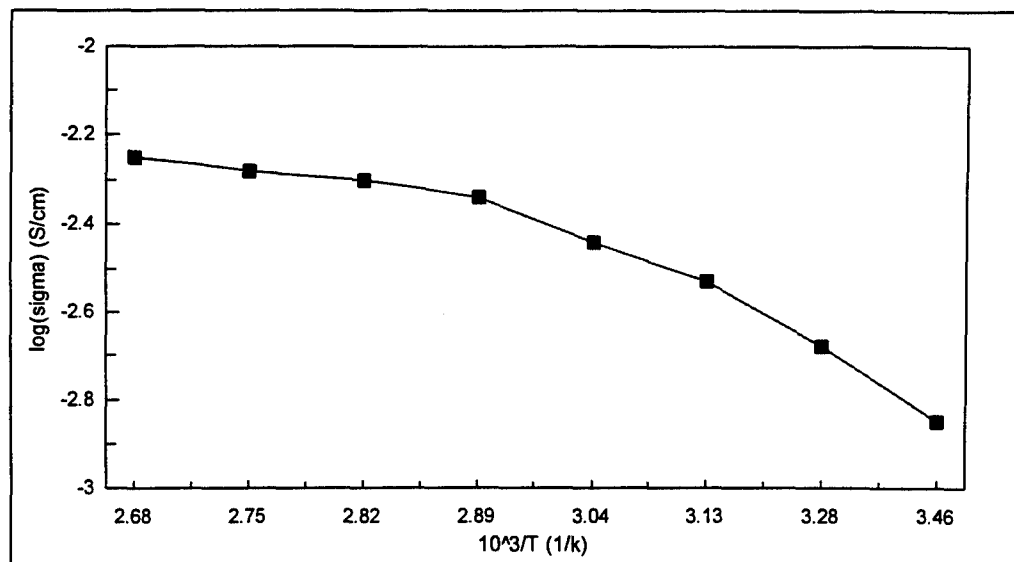


Figure 10. Conductivity as a function of temperature, as an Arrhenius plot, for the film of formulation PA3

3.5 CYCLIC VOLTAMMETRY RESULTS OF $\text{Li}_5\text{Sb}_5\text{P}_2\text{O}_{20}$

Electrochemical stability of the lithium phosphatoantimonate was investigated by cyclic voltammetry. For this purpose a liquid electrolyte solution containing the solvents and the supporting electrolyte salt (LiTFMSI) was first prepared. Cyclic voltammetry scans were taken using 1 cm² area platinum working and counter electrodes and a lithium reference electrode. The test was carried out at 10 mV/second scan rate in the potential range of +0.1 V to +4.0 V vs Li⁰ reference electrode. A limit of +0.1 V vs Li⁰ reference electrode was selected to prevent lithium deposition and its consequent incorporation into the platinum working electrode. A limit of +4 V vs Li⁰ reference was used to cover the stability test of the electrolyte for a 4 V lithium cell with an appropriate cathode.

The cyclic voltammogram, shown in Figure 11, was obtained for the solvents alone. The few peaks noted were attributed to catalytic waves due some unknown impurities in the solvents used, as the magnitude of current is not significant. This voltammogram served as the base line for the investigation of stability of the lithium phosphatoantimonate. Next, $\text{Li}_5\text{Sb}_5\text{P}_2\text{O}_{20}$ was added to the test solution and the cyclic voltammetry scan was taken under similar experimental conditions. The result shown in Figure 12 was observed. The cyclic voltammograms with and without the $\text{Li}_5\text{Sb}_5\text{P}_2\text{O}_{20}$ were identical. These results have indicated that the $\text{Li}_5\text{Sb}_5\text{P}_2\text{O}_{20}$ was stable in the potential range of a 4V lithium battery for BMDO applications.

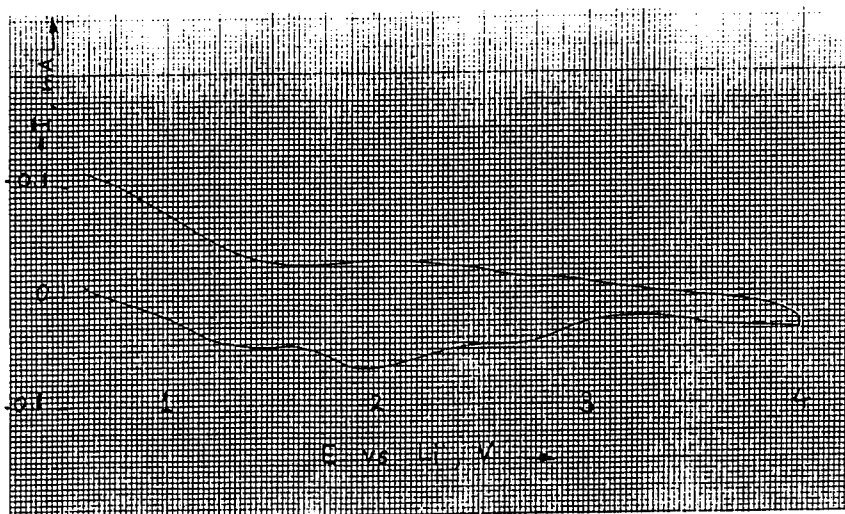


Figure 11. Cyclic voltammogram using 1 cm² area platinum counter and working electrodes and a lithium reference electrodes in a solution of LiN-(SO₂CF₃)₂ in a solvent mix of γ -butyrolactone, dibutyl phthalate, ethylene carbonate and 3-methyl-2-oxazolidinone.

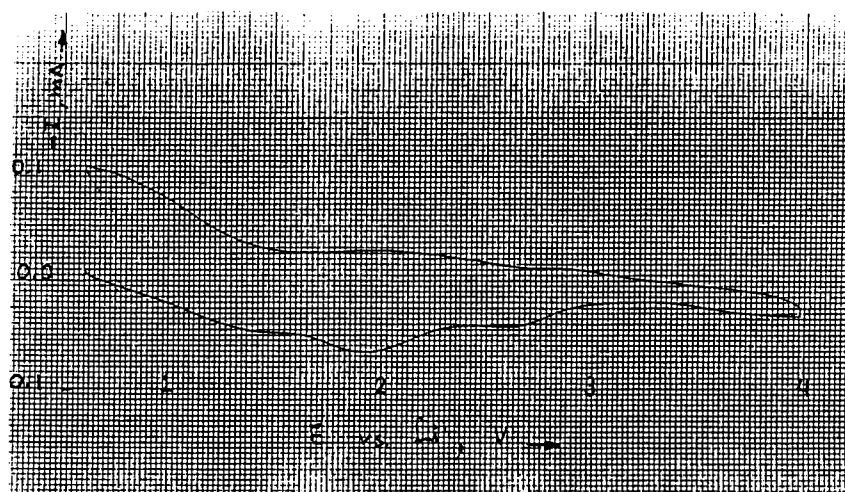


Figure 12. Cyclic voltammogram using 1 cm² area platinum counter and working electrodes and a lithium reference electrodes in a solution of LiN-(SO₂CF₃)₂ in a solvent mix of γ -butyrolactone, dibutyl phthalate, ethylene carbonate and 3-methyl-2-oxazolidinone, containing a dispersion of Li₅Sb₅P₂O₂₀.

3.6. PERFORMANCE PROJECTION

For the purpose of analyzing and projecting the performance, a preliminary design calculation for a 24 volt, 5 Ah battery is made for space power applications. The battery system calculations are made for a $\text{Li}_x\text{C}/\text{MnO}_2$ electrochemical system. Table 7 lists projected weights and thicknesses of cell components for a 5 Ah capacity, 500 cm^2 active area. Incidentally, these weights and thicknesses are based on experimental data from another Technochem SBIR Phase I Program on a polymer electrolyte lithium battery. The overall cell dimension of $25\text{ cm} \times 25\text{ cm}$ will accommodate a cell active area of 500 cm^2 . Eight cells in a bipolar configuration will supply the 24 V requirement. Projected battery weight and volume are estimated at 540 g and 0.310 L. Thus, the specific energy and energy density are 222 Wh/kg and 387 Wh/L. If the electrode weights can be reduced by 30% by further optimization, compared to the experimental values, the projection for the battery weight and volume are 360 g and 0.30 L. For this projection, a specific energy of 333 Wh/kg and an energy density of 400 Wh/L are estimated.

For projecting the power performance of the design concept, polymer electrolyte conductivity achieved in this program of $5 \times 10^{-3}\text{ S/cm}$ is used. The cell polarization of two times the electrolyte resistance is assumed. For the electrolyte separator thicknesses of 50, 100 and 200 micrometers, the cell voltage versus current density for the 500 cm^2 active area cell is presented in Figure 13. For the 8-cell bipolar battery pack of nominal 24 V system, the delivered power versus discharge current is presented in Figure 14. With 100 μm thick separators, the projected specific power and power density for a BMDO application are estimated at 4.2 kW/kg and 5 kW/L, respectively.

Table 7 Projected weights and thicknesses of 500 cm^2 area cell electrodes and components

Component	Weight, g	Thickness, mm	Remarks
Anode	10	0.15	Li intercalation
Cathode	20	0.16	0.1 Ah/g MnO_2
Electrolyte	20	0.10	PAN or PVDF
Bipolar film	10	0.20	carbon plastic
Total	60	0.61	

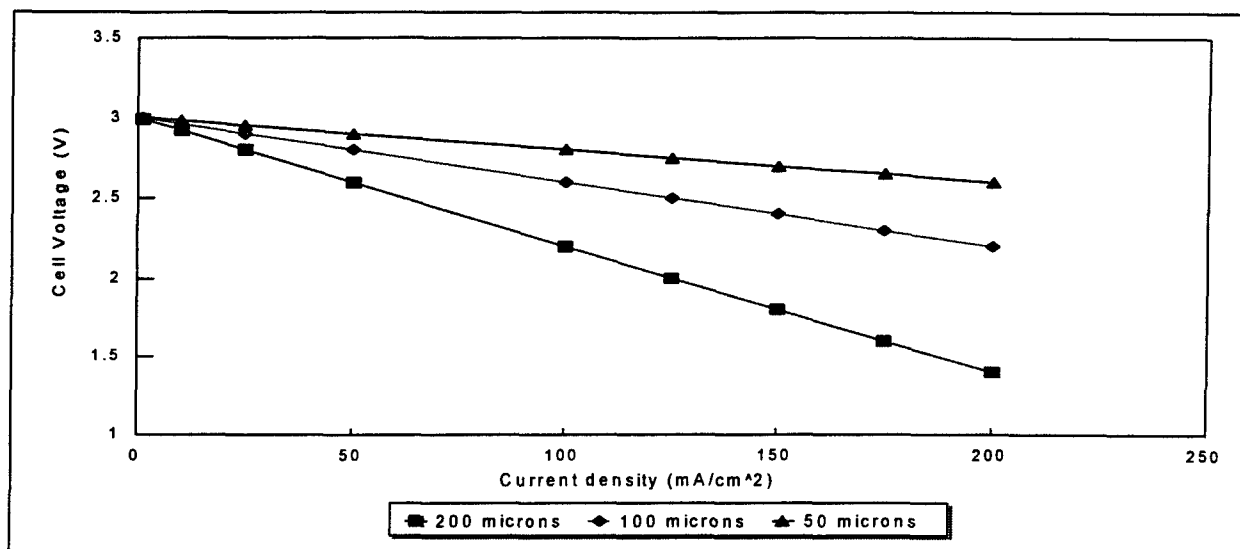


Figure 13. Cell voltage versus current density for a projected 500 cm² area cell with a 200 ohm cm resistivity electrolyte assuming a cell polarization of 2 x IR for the three thicknesses of the electrolyte separator.

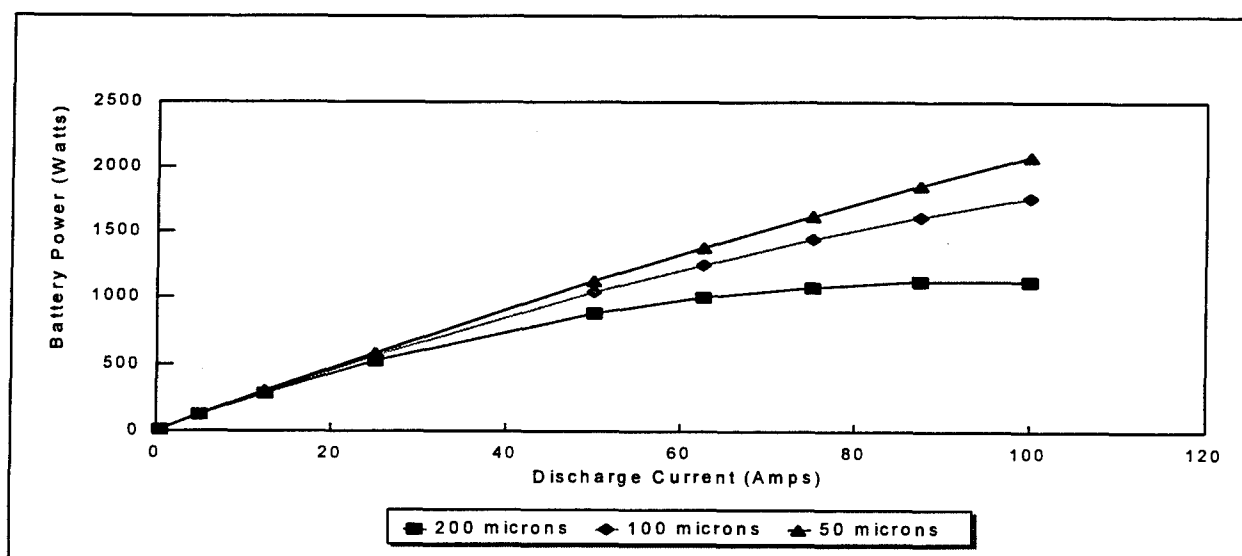


Figure 14. Projected power performance for an 8-cell bipolar 24-V Li_xC/MnO₂ battery system using 200 Ωcm resistivity electrolyte separators of three different thicknesses, assuming a cell polarization of twice the IR-drop.

3.7. CONCLUSIONS - CONDUCTIVITY IMPROVEMENT SCHEMES

Table 8 summarizes the results obtained for various approaches utilized to improve the conductivity of electrolyte separator materials. Conclusions which can be drawn from these efforts are summarized below.

1. $\text{Li}_5\text{Sb}_5\text{P}_2\text{O}_{20}$ compound in combination with another fine particulate inorganic ionic conductor, namely, Li_5AlO_4 did not result in increasing the conductivity at elevated temperatures.
2. Substituting niobium for antimony in $\text{Li}_5\text{Sb}_5\text{P}_2\text{O}_{20}$, $\text{Li}_3\text{Sb}_3\text{P}_2\text{O}_{14}$ and LiSbP_2O_8 compounds yielded electrolytes that had lower ionic conductivities. The phosphatoniobate structures could not be identified and appeared to be too complex.
3. Partial substitution of antimony in the phosphatoantimonates by germanium (IV), which is expected to create defects in the crystal structures, also did not yield improved conductivities.
4. It is anticipated that high temperature (400-500°C) batteries will have limited applications due to number of difficulties encountered in fabrication and operation of these systems. Hence, battery systems operating in the range of 75 to 150°C will have wider application in meeting the BMDO requirements.
5. The use of the $\text{Li}_5\text{Sb}_5\text{P}_2\text{O}_{20}$ phosphatoantimonate and supporting electrolyte in a polymer matrix looks quite promising as a electrolyte separator for lithium ion batteries.
6. Polymer electrolytes containing $\text{Li}_5\text{Sb}_5\text{P}_2\text{O}_{20}$ have conductivities of $> 5 \times 10^{-3} \text{ S/cm}$ at 100°C and are mechanically stable without undergoing significant amount of creep at these high temperatures.
7. The new electrolyte, $\text{Li}_5\text{Sb}_5\text{P}_2\text{O}_{20}$ synthesized in this program is electrochemically stable from 0.1 to +4 V with respect to lithium.
8. Performance projection for a 24-V, 500 cm^2 active area $\text{Li}_x\text{C}/\text{MnO}_2$ battery using the developed electrolyte separators is estimated to deliver a specific energy of 333 Wh/kg and an energy density of 400 Wh/L. The projected specific power and power density for this design are estimated at 4.2 kW/kg and 5 kW/L, respectively.
9. The electrolyte separator development needs to be utilized in $\text{Li}_x\text{C}/\text{MnO}_2$ battery. Design, development, optimization, fabrication, and testing of the cell and battery components need to be carried out in a Phase II program.

Table 8 Conductivity values for electrolyte separators of various combinations

Compound/Film Formulation	Wafer/Film components	Thickness of Wafer/Film* (mm)	Conductivity (S/cm)
Samples in Compacted Powder (Wafer) Form			
Li ₅ Sb ₅ P ₂ O ₂₀ and Li ₅ AlO ₄	20 wt% Li ₅ AlO ₄	0.730	1.1x10 ⁻³ @475°C
Li ₅ Nb ₅ P ₂ O ₂₀		0.485	5.1x10 ⁻⁴ @498°C
Li ₅ Nb ₃ P ₂ O ₁₄		0.470	3.2x10 ⁻⁴ @498°C
Li ₅ Ge ₄ SbP ₂ O ₂₀		0.620	3.6x10 ⁻⁵ @398°C
Li ₇ Ge ₂ Sb ₃ P ₂ O ₁₄		0.633	3.4x10 ⁻⁵ @442°C
Samples in Polymer Film Form			
PV1	PVdF,DBP,DMF,PC,LiTFMSI, Li ₅ Sb ₅ P ₂ O ₂₀	0.140	3.7x10 ⁻³ @140°C
PV2	PVdF,DBP,DMF,PC, LiTFMSI, Li ₅ Sb ₅ P ₂ O ₂₀ , LiAlO ₄	0.250	8.3x10 ⁻⁴ @140°C
PA1	PAN, EC, PC, GBL, MOZ, LiTFMSI, Li ₅ Sb ₅ P ₂ O ₂₀	0.136	2.4x10 ⁻³ @140°C
PA2	PAN, EC, PC, DBP, GBL, MOZ, LiTFMSI, Li ₅ Sb ₅ P ₂ O ₂₀ , cab-o-sil	0.247	5.6x10 ⁻³ @100°C
PA3	PAN, EC, PC, DBP, GBL, MOZ, LiTFMSI, Li ₅ Sb ₅ P ₂ O ₂₀ , cab-o-sil	0.222	5.6x10 ⁻³ @100°C

*Thickness of polymer films were measured after heating the film

SECTION 4

CONCLUSIONS AND RECOMMENDATIONS

Following conclusions can be drawn from the Phase I effort.

- New Li^+ ion conductors based on lithium phosphatoantimonates have been developed. These compounds can be prepared in high purity and good yield.
- The phosphatoantimonate compounds of potassium, KSbP_2O_8 , $\text{K}_3\text{Sb}_3\text{P}_2\text{O}_{14}$ and $\text{K}_5\text{Sb}_5\text{P}_2\text{O}_{20}$ can be synthesized by solid-state reaction. These compounds have interesting crystal structures for ion exchange and ionic conduction.
- The corresponding lithium salts of these compounds cannot be prepared directly by solid-state reaction. The lithium phosphatoantimonates can be made from the phosphatoantimonic acid by an acid-base titration. These lithium salts retain the same crystal structure habits as those for the corresponding potassium salts with minor changes in crystallographic lattice parameters.
- The lithium phosphatoantimonates, Li_3 and Li_5 type, exhibit a linear behavior for conductivity with temperature. The conductivity of these materials is about 3×10^{-3} s/cm.
- Ionic conductivity decreases from $\text{Li}_5\text{Sb}_5\text{P}_2\text{O}_{20}$ to LiSbP_2O_8 , i.e., $\sigma(\text{Li}_5\text{Sb}_5\text{P}_2\text{O}_{20}) > \sigma(\text{Li}_3\text{Sb}_3\text{P}_2\text{O}_{14}) > \sigma(\text{LiSbP}_2\text{O}_8)$.
- Lithium phosphatoantimonate compounds, $\text{Li}_5\text{Sb}_5\text{P}_2\text{O}_{20}$ in particular, is suitable for batteries that operate at 400-500°C.
- $\text{Li}_5\text{Sb}_5\text{P}_2\text{O}_{20}$ compound in combination with another fine particulate inorganic ionic conductor, namely, Li_5AlO_4 did not result in increasing the conductivity at elevated temperatures.
- Partial substitution of antimony in the phosphatoantimonates by germanium (IV), which is expected to create defects in the crystal structures, also did not yield improved conductivities.
- It is anticipated that high temperature (400-500°C) batteries will have limited applications due to number of difficulties encountered in fabrication and operation of these systems. Hence, battery systems operating in the range of 75 to 150°C will have wider application in meeting the BMDO requirements.

- The use of the $\text{Li}_5\text{Sb}_5\text{P}_2\text{O}_{20}$ phosphatoantimonate and supporting electrolyte in a polymer matrix looks quite promising as a electrolyte separator for lithium ion batteries.
- Polymer-gel electrolytes containing $\text{Li}_5\text{Sb}_5\text{P}_2\text{O}_{20}$ have conductivities of $> 5 \times 10^{-3} \text{ S/cm}$ at 100°C and are mechanically stable without undergoing significant amount of creep at these high temperatures.
- The new electrolyte, $\text{Li}_5\text{Sb}_5\text{P}_2\text{O}_{20}$ synthesized in this program is electrochemically stable from 0.1 to +4 V with respect to lithium. These compounds can provide good thermal and mechanical stability for a thin solid polymer electrolyte separator for pulse power batteries that can be operated at $75\text{-}150^\circ\text{C}$.
- Performance projection for a 24-V, 500 cm^2 active area $\text{Li}_x\text{C}/\text{MnO}_2$ battery using the developed electrolyte separators is estimated to deliver a specific energy of 333 Wh/kg and an energy density of 400 Wh/L . The projected specific power and power density for this design are estimated at 4.2 kW/kg and 5 kW/L , respectively.

Based on the Phase I effort, following recommendations are offered:

- A superior performance lithium pulse power battery can be developed utilizing an optimized thin film electrolyte of high conductivity, in combination with (i) a high rate lithium intercalation anode, and (ii) a suitable MnO_2 cathode.
- Based on conductivity of 5×10^{-3} at $90\text{-}100^\circ\text{C}$ in a PAN polymer supporting matrix, the thin polymer electrolyte separator, using $\text{Li}_5\text{Sb}_5\text{P}_2\text{O}_{20}$, of 500 cm^2 area and $0.5\text{-}0.8 \text{ mm}$ thickness in a Li/MnO_2 battery is capable of delivering 200 watts power.
- Therefore, the Phase I developments need to be further optimized, and design, development, fabrication and test-validation of cells and prototypes in a Phase II program are warranted.

REFERENCES

1. E. J. Plichta and W. K. Behl, J. Electrochem. Soc. **139**, 1509, (1992)
2. E. J. Plichta and W.K. Behl, J. Electrochem. Soc. to be published.
3. E. E. Hellstrom and W. van Gool, Solid State Ionics **2**, (1981) 53.
4. R. M. Biefeld and R. T. Johnson, Jr, J. Electrochemical Soc. **126**, (1979) 1.
5. J. H. Jackson and D. A. Young, J. Phys. Chem. Sol. **30**, (1969) 1973.
6. A. M. Glass and K. Nassau, J. appl. Phys. **51**, (1980) 3756.
7. W. Weppner and R. A. Huggins, J. Electrochem. Soc. **124**, (1977) 35.
8. P. Hartwig, W. Weppner, and W. Wichelhaus, Mat. Res. Bull. **14**, (1979) 493.
9. H. Y. -P. Hong, Mat. Res. Bull. **13** (1978) 117; U. Alpen, M. F. Bell, W. Wichelhaus, Y. Cheung, and G. F. Dudley, Electrochim. Acta **23** (1978) 1395.
10. Y. W. Hu, I. D. Raistrick, and R. A. Huggins, J. Electrochem. Soc. **124** (1977) 1240.
11. M. S. Whittingham and R. A. Huggins in Solid State Chem., eds. R. S. Roth and S. J. Schneider, NBS Spec. Publ. 364 (Natl. Bureau of Standards, Washington, D. C., (1972) 139.
12. P. A. G. O'hare and G. K. Johnson J. Chem. Thermodyn. **7** (1975) 13.
13. R. M. Yonco, E. Veleckis, and V. A. Maroni J. Nucl. Mat. **57** (1975) 317.
14. J. P. Jolivet and J. Lefebvre Bull. Soc. Chim. (1975) 2409.
15. N. G. Chernorrukov, I. A. Korshunov, N. P. Egorov, A. I. Zabelin, and T. A. Galanova Izv. Akad. Nauk. SSSR, Neorg. Mater. **17(6)** (1981) 1058.
16. N. G. Chernorrukov, N. P. Egorov, and T. A. Galanova Izv. Akad. Nauk. SSSR, Neorg. Mater. **17(2)** (1981) 328.
17. A. Winkler and E. Thilo Z. Anorg. Allg. Chem. **346** (1966) 92.
18. A. Winkler and E. Thilo J. Polymer. Sci. **16** (1969) 4283.

19. Y. Piffard, and A. Lachgar, *J. Solid State Chem.*, **60** (1985) 209.
20. A. Lachgar, Y. Piffard, and M. Tournoux *Mat. Res. Bull.*, **20**, (1985) 715.
21. Y. Piffard, A. Lachgar, and M. Tournoux *J. Solid State Chem.*, **58**, 253 (1985) 253.
22. M.B. Armand, J.M. Chabagna, and M.J. Duclot, Second Internet Symp. Solid Electrolyte, St. Andrews, Scotland, paper 6.5 (1979)
23. K.M. Abraham in *Application of Electroactive Polymer*, Ed. Scrosati, Chapman & Hall, London, p. 75 (1993).
24. D. Davous, B. Sebile, *Europ. Polym. J.* 16, 347, (1980)
25. K.M. Abraham, M. Alamgir, *J. Electrochem. Soc.* 137, 1657, (1990)
26. H. Hong, C. Liqun, H. Hoejie, X. Rongjian, *Electrochim Acta* 37, 1671, (1992)
27. R. Huq, R. Kokslang, P.E. Tonder, G. C > Farrington, *Electrochim Acta*, 37, 1681, (1992); *Solid State Ionics* 57, 277, (1992)
28. P.S. Prasad, B.B. Owens, W.H. Smyrl, A. Selvaggi, B. Scrosati, in *Recent Advances in Fast Ion Conducting Materials and Devices*. Eds. B.V.R. Chowdari, Q.G. Liu, L.Q. Chin, World Scientific Singapore, P. 1709 (1990)
29. J.P. Southall, A.M. Voice, V. Rogers, G.R. Davies, J.M. McIntyre, I.M. Ward, in *Seventh International Meeting on Lithium Batteries*, Boston, paper no. I-B-26 (1994)
30. G.B. Appetecchi, F. Croce, B. Scrosati, In *Proceedings of the 36th Power Sources Conference*, p 236 (1994).
31. M. Alamgir, K.M. Abraham, in *Seventh International Meeting on Lithium Batteries*, Boston, extended abstract page 58 (1994)
32. M.B. Armand in *New Electrolyte salts for Lithium Batteries*, ECS Symposium Cleveland Section (1993)
33. J.M. Tarascon and D. Guyomard, *J. Electrochem. Soc.* 139, 937 (1992)

DISTRIBUTION LIST

AUL/LSE

Bldg 1405 - 600 Chennault Circle
Maxwell AFB, AL 36112-6424

1 cy

DTIC/OCP

8527 John J. Kingman Rd, Suite 0944
Ft Belvoir, VA 22060-6218

2 cys

AFSAA/SAI

1580 Air Force Pentagon
Washington, DC 20330-1580

1 cy

PL/SUL

Kirtland AFB, NM 87117-5776

2 cys

PL/HO

Kirtland AFB, NM 87117-5776

1 cy

Official Record Copy

PL/VTP/Lt Rainbow
Kirtland AFB, NM 87117-5776

2 cys

PL/VT

Dr Wick
Kirtland AFB, NM 87117-5776

1 cy